IECM Technical Documentation:

Technical Performance and Environmental Impact of Co-Firing Power Plants

November 2024

IECM Technical Documentation:
Technical Performance and Environmental Impact of Co-Firing Power Plants

(Preliminary Version)

Prepared by:
Wanying Wu and Haibo Zhai
The Integrated Environmental Control Model Team
University of Wyoming
Laramie, WY 82071
www.uwyo.edu/iecm

November 2024

Table of Content

Introduction ... 5
Section 1: Fuel Database ... 5
1.1 Nomenclature ... 5
1.2 Fuel Blend ... 6
1.3 Fuel Property ... 6
1.4 Fuel Cost ... 10
Section 2: Boiler Efficiency Algorithm ... 13
2.1 Nomenclature ... 13
2.2 Boiler Efficiency ... 14
2.3 Type of Heat Loss ... 14
(a) Heat Loss from Dry Flue Gas ... 14
(b) Heat Loss from Water Vapor ... 14
(c) Heat Loss from Unburned Carbon and Carbon Monoxide ... 15
(d) Heat Loss from Ash ... 16
(e) Heat Loss from Radiation Exchange ... 17
(f) Unaccounted Loss ... 17
Section 3: Life Cycle Greenhouse Gas Emission Model ... 18
3.1 Nomenclature ... 18
3.2 Analysis Scope and Method ... 23
3.3 Greenhouse Gas Emissions by Stage ... 24
(a) Fuel Supply ... 24
(b) Combustion-Based Power Generation ... 41
(c) CO_2 Transport and Storage ... 41
Section 4: Case Study ... 44
4.1 Input Parameter and Assumption ... 44
4.2 Major Result ... 45
(a) PC Power Plants without and with CCS ... 45
(b) Coal-Biomass Co-Firing Power Plants without and with CCS ... 46
(c) Breakeven Biomass Co-Firing Level for Net-Zero Emissions ... 48
Summary ... 50
References ... 50
Appendix ... 59
Appendix 1 Fuel Property of Coal, Waste Coal, and Biomass. ... 59
Appendix 2 GWP Value and Emission Intensity Associated with Consumption of Electricity, Diesel, and Steel ... 64

List of Figures

Figure 3.1. Life Cycle Boundary of Power Plant with Carbon Capture and Storage. 24
Figure 4.1. Performance of 20% Co-Firing Power Plants. 46
Figure 4.2. Life Cycle Emissions of Co-Firing Power Plants……………………………………47
Figure 4.3. Life Cycle Emissions Distribution of Co-Firing Power Plants. 48
Figure 4.4. Breakeven Co-Firing Level for Achieving Net-Zero Life Cycle Emissions............. 49

List of Tables

Table 1.1. As-Received Coal Property. 7
Table 1.2. As-Received Waste Coal Property. 8
Table 1.3. As-Received Biomass Property. 9
Table 1.4. As-Delivered Waste Coal Cost. 10
Table 1.5. As-Delivered Biomass Cost. 12
Table 2.1 Specific Heat of Ash. 16
Table 3.1. Inputs of Coal Mining and Processing Emission Estimation. 26
Table 3.2. Coal Supply Chain Emissions... 26
Table 3.3. Inputs of Waste Coal Extraction and Processing Emission Estimation....................... 28
Table 3.4. Waste Coal Supply Chain Emissions.. 28
Table 3.5. Inputs of Land Use Change Emission Estimation. 33
Table 3.6. Inputs of CO_2 Uptake Estimation. 35
Table 3.7. Inputs of Biomass Cultivation Emission Estimation 36
Table 3.8. Inputs of Biomass Harvesting Emission Estimation.. 37
Table 3.9. Inputs of Biomass Processing Emission Estimation.. 38
Table 3.10. Biomass Supply Chain Emissions. 38
Table 3.11. Inputs of CO_2 Transport and Storage Emission Estimation. 42
Table 3.12. CO_2 Transport and Storage Emissions... 43
Table 4.1. Major Parameters and Assumptions for Case Study. 44

Acknowledgments

This research is supported by the U.S. Department of Energy's Office of Fossil Energy and Carbon Management (Project Number DE-FE0032193). Any opinions, findings, conclusions, or recommendations expressed in this material are those of the authors alone and do not reflect the views of any government agency.

Introduction

The Integrated Environmental Control Model (IECM) can simulate the performance, emissions, and cost of various conventional and advanced coal-fired power plants under a variety of scenarios. With growing interest in low-carbon technologies, coal-biomass co-firing stands out as a promising Bioenergy with Carbon Capture and Storage (BECCS) technology for assisting carbon mitigation in the energy sector. This report outlines the refinements and additions made to IECM version 11.5. These updates enhance the IECM's capability to simulate the technical performance and environmental impact of co-firing power plants. Accordingly, the updates are presented in four main sections:

- Section 1 Fuel Database
- Section 2 Boiler Efficiency Algorithm
- Section 3 Life Cycle Greenhouse Gas Emission Model
- Section 4 Case Study

Section 1: Fuel Database

This section consists of 4 parts: (1) "Nomenclature" shows the symbol for the parameter in formulas, (2) "Fuel Blend" explains the calculation method used for determining the property and cost of blended fuel, (3) "Fuel Property" exhibits the newly added properties of coal, waste coal, and biomass, and (4) "Fuel cost" displays the estimation methods for the default as-delivered costs.

1.1 Nomenclature

Symbol

ARB	fuel property on an as-received basis (wt.% or kJ/kg)
ADC_{HP}	as-delivered hybrid poplar cost (2007$/tonne)
ADC_m	mass-based as-delivered cost ($/tonne)
ADC_{SG}	as-delivered switchgrass cost (2007$/tonne)
ADC_{TW}	as-delivered torrefied wood cost (2018$/tonne)
CapC	capital cost of the torrefaction plant (2018$)
CCF	capital charge factor of the torrefaction plant (fraction/year)
CF	capacity factor of the torrefaction plant (%)
CPIA	consumer price index in year A
CPIB	consumer price index in year B
DB	fuel property on a dry basis (wt.% or kJ/kg)
EC	annual electricity consumption cost of the torrefaction plant (2018$/year)
F_{AR}	as-received basis fuel consumption rate of power plant (short-ton/day)
F_D	dry basis fuel consumption rate of power plant (short-ton/day)
F^{MMBtu}	unit conversion between Btu and MMBtu, with a value of 10^{-6} (MMBtu/Btu)
F^{STtlb}	unit conversion between short-ton and pound, with a value of 2000 (lb/short-ton)
F^{STtMT}	unit conversion between short-ton and tonne, with a value of 1.1023 (short-ton/tonne)
FC_m	mass-based feedstock cost ($/short-ton)
FC_e	arithmetic mean of the energy-based feedstock cost ($/MMBtu)
HA	adjusted hydrogen content, which excludes H in the sample moisture (wt.%)
HB	hydrogen content, which includes H in the sample moisture (wt.%)
HHV_{eu}	higher heating value (Btu/lb)

LHV_{eu}	lower heating value (Btu/lb)
M	moisture content on an as-received basis (wt.%)
NGC	annual natural gas consumption cost of the torrefaction plant (2018$/year)
OA	adjusted oxygen content, which excludes O in the sample moisture (wt.%)
OB	oxygen content, which includes O in the sample moisture (wt.%)
OMC	annual operation and maintenance cost of the torrefaction plant (2018$/year)
PR	production rate of torrefied wood (short-ton/day)
RDA	constant dollar in year A
RDB	constant dollar in year B
TC_{TW}	transport cost of torrefied wood (2018$/tonne)
TC_m	mass-based transport cost ($/tonne/km)
TD	transport distance (km)
WC	annual raw wood consumption cost of the torrefaction plant (2018$/year)

1.2 Fuel Blend

The fuel blend function allows the user to include up to three individual fuels for combustion. The properties and cost of the blended fuel are determined using the mass-based ratio of the individual fuels. When the input fuel is not coal, the IECM model uses the properties of the input fuel to select the most similar coal as a proxy for calculating plant performance. We suggest that the mass percentage of coal in a blended fuel be at least 60%.

1.3 Fuel Property

The fuel type in the fuel database is expanded to include not only coal, but also waste coal and biomass. The structure of the database is enhanced to include proximate analysis data in addition to heating value, ultimate analysis data, and ash property. The fuel properties are derived from various literature and are specified as follows. The fuel properties in the IECM are presented on an as-received basis, with adjustments made using Equations (1.1) to (1.3) if the collected data is not aligned with this basis.

The properties for the following coals are expanded to include proximate analysis data: Appalachian Medium Sulfur (bituminous), Illinois No. 6 (bituminous), Upper Freeport (bituminous), Wyoming Powder River Basin (subbituminous), and North Dakota Lignite (lignite). The properties of coal samples are gathered from technical reports of the IECM, the National Energy Technology Laboratory (NETL), and the Electric Power Research Institute (EPRI) (IECM, 2019a; NETL, 2007, 2019; EPRI, 2008, 2018). Table S1.1 displays the collected properties for five coal samples.

Waste coal is a new fuel type with three samples from the Illinois Basin. They are Herrin Refuse Coal Mach #1, Herrin Refuse Lively Grove Coal, and Dekoven Refuse Coal Eagle River #1. The properties of waste coal samples are collected from Kolker et al. (2021). Table S1.2 shows the collected properties for three waste coal samples.

Biomass is another new fuel type with seven samples, including Switchgrass, Miscanthus, Hybrid Poplar, Torrefied Wood, Corn Stover, Wheat Straw, and Pine Spruce Chips. Those samples are classified into three categories: energy crop, agricultural residue, and forestry residue. The categorization of the samples is shown in the table below. The properties of biomass are gathered from multiple sources, including technical reports from the EPRI and the NETL, the Energy Research Centre of the Netherlands (ECN) database, and published papers (Bush et al., 2001; ECN, 2022; EPRI, 2010, 2012; Zygarlicke et al., 2001; Bridgeman et al., 2010). Tables S2 and S3 present the collected properties for seven biomass samples.

To ensure consistency of fuel properties in the IECM's fuel database, adjustments are made to the collected properties where necessary, following the methodology provided by Riley (2014). Equation (1.1) converts fuel properties to an as-received basis. Equations (1.2) and (1.3) adjust the hydrogen and oxygen contents by excluding moisture-related components. Tables 1.1–1.3 summarize the fuel properties of coal, waste coal, and biomass embedded into the IECM, respectively.

Note that for biomass with more than 20 wt.% moisture content, a drying process must be considered. If on-site drying is applied, the associated cost and parasitic load should be accounted for in the plant-level economic and performance calculations.

$$\mathrm{ARB} = \mathrm{DB} \times \frac{100 - \mathrm{M}}{100} \tag{1.1}$$

$$\mathrm{HA} = \mathrm{HB} - \mathrm{M} \times \frac{2}{18} \tag{1.2}$$

$$\mathrm{OA} = \mathrm{OB} - \mathrm{M} \times \frac{16}{18} \tag{1.3}$$

Table 1.1. As-Received Coal Property.

Coal Rank			**Bituminous**			**Subbituminous**	**Lignite**
Feedstock Name			**Pittsburgh #8 (Appalachian Medium Sulfur)**[1]	**Illinois No.6**	**Upper Freeport (NETL)**	**Wyoming Powder River Basin**	**North Dakota Lignite**
Fuel Property	Higher Heating Value	kJ/kg	308423	27135	30980	19399	14003
	Carbon	wt.%	73.81	63.75	73.39	48.18	35.04
	Hydrogen	wt.%	4.88	4.5	4.03	3.31	2.68
	Oxygen	wt.%	5.41	6.88	4.79	11.87	11.31
	Chlorine	wt.%	0.06	0.29	0.00	0.01	0.09
	Sulfur	wt.%	2.13	2.51	2.29	0.37	1.16
	Nitrogen	wt.%	1.42	1.25	1.33	0.7	0.77
	Ash	wt.%	7.24	9.7	13.03	5.32	15.92
	Moisture	wt.%	5.05	11.12	1.13	30.24	33.03
Proximate Analysis	Moisture	wt.%	5.05	11.12	1.13	30.24	33.03
	Ash	wt.%	7.24	9.7	13.03	5.32	15.92
	Volatile Matter	wt.%	40.37	34.99	29.43	31.39	27.17

	Fixed Carbon	wt.%	47.34	44.19	56.41	33.05	23.89
Ash Property	SiO_2	wt.%	54.50	46.80	44.80	63.19	45.16
	Al_2O_3	wt.%	17.30	18.00	24.10	30.00	21.91
	Fe_2O_3	wt.%	4.50	20.00	17.30	2.90	6.97
	CaO	wt.%	10.70	7.00	4.20	0.91	16.42
	MgO	wt.%	2.40	1.00	1.60	0.76	3.26
	Na_2O	wt.%	1.48	0.60	0.00	0.38	0.78
	K_2O	wt.%	1.11	1.90	2.70	1.49	0.80
	TiO_2	wt.%	0.70	1.00	1.30	0.09	1.63
	MnO_2	wt.%	0.00	0.00	0.00	0.00	0.00
	P_2O_5	wt.%	0.27	0.20	0.10	0.08	0.81
	SO_3	wt.%	7.04	3.50	3.90	0.20	1.26
	Other	wt.%	0.00	0.00	0.00	0.00	1.00

Footnote:
1. Fuel properties are adjusted to an as-received basis using Equations (1.1) from the values reported in Table S1.1.

Table 1.2. As-Received Waste Coal Property.

Mining Approach			**Underground**		**Surface**
Feedstock Name			**Herrin Refuse Coal Mach #1**	**Herrin Refuse Coal Lively Grove Coal**	**Dekoven Refuse Coal Eagle River #1**
Fuel Property	Higher Heating Value	kJ/kg	4133	4617	17496
	Carbon	wt.%	10.47	11.09	39.04
	Hydrogen[1]	wt.%	1.07	1.20	2.85
	Oxygen[2]	wt.%	2.99	2.53	2.21
	Chlorine	wt.%	0.00	0.00	0.00
	Sulfur	wt.%	3.57	3.23	9.4
	Nitrogen	wt.%	0.42	0.41	0.93
	Ash	wt.%	73.84	73.64	40.90
	Moisture	wt.%	7.64	7.90	4.67
Proximate Analysis	Moisture	wt.%	7.64	7.90	4.67
	Ash	wt.%	73.84	73.64	40.90
	Volatile Matter	wt.%	10.42	9.73	25.05
	Fixed Carbon	wt.%	8.10	8.73	29.38

Ash Properties	SiO_2	wt.%	56.51	61.04	44.51
	Al_2O_3	wt.%	16.07	17.46	14.17
	Fe_2O_3	wt.%	8.70	7.79	30.52
	CaO	wt.%	4.25	0.95	1.62
	MgO	wt.%	1.53	1.64	0.91
	Na_2O	wt.%	0.87	1.16	0.42
	K_2O	wt.%	3.20	2.68	2.10
	TiO_2	wt.%	0.80	0.81	0.77
	MnO_2	wt.%	0.00	0.00	0.00
	P_2O_5	wt.%	0.50	0.37	0.26
	SO_3	wt.%	0.00	0.00	0.00
	Other[3]	wt.%	7.57	6.10	4.72

Footnotes:
1. Hydrogen weight percentage is adjusted using Equation (1.2) from the value reported in Table S1.2;
2. Oxygen weight percentage is adjusted using Equation (1.3) from the value reported in Table S1.2;
3. The Other value is adjusted so that the total sum is 100%.

Table 1.3. As-Received Biomass Property.

Category			**Energy Crop**				**Agricultural Residue**		**Forestry Residue**
Feedstock Name			**Switchgrass[1]**	**Miscanthus**	**Hybrid Poplar**	**Torrefied Wood [2,3]**	**Corn Stover [1]**	**Wheat Straw[3]**	**Pine Spruce Chips[1]**
Fuel Property	Higher Heating Value	kJ/kg	17159	16001	17773	23395	16230	16686	19305
	Carbon	wt.%	42.04[4]	40.36[4]	45.03[4]	57.93[4]	41.24	43.00[4]	47.91[4]
	Hydrogen	wt.%	5.21	4.92	5.55[5]	5.57	5.15	6.08	5.58
	Oxygen	wt.%	37.59	37.19	42.01[6]	32.10	36.51	38.62	37.04
	Chlorine	wt.%	0.00	0.05	0.01	0.00	0.09	0.23	0.00
	Sulfur	wt.%	0.15	0.05	0.25	0.00	0.09	0.08	0.03
	Nitrogen	wt.%	0.86	0.28	0.82	0.50	0.59	0.35	0.61
	Ash	wt.%	4.94	2.61	1.13	1.80	10.68	4.86	2.52
	Moisture	wt.%	9.21	14.54	5.20	2.10	5.65	6.78	6.31
Proximate Analysis	Moisture	wt.%	9.21	14.54	5.20	2.10	5.65	6.78	6.31
	Ash	wt.%	4.94	2.61	1.13	1.80	10.68	4.86	2.52
	Volatile Matter	wt.%	75.41	72.12	78.85	66.90	70.10	75.92	71.86

	Fixed Carbon	wt.%	10.44	10.73	14.82	29.20	13.57	12.44	19.31
Ash Properties	SiO_2	wt.%	55.64	61.84	4.60	6.24	53.74[7]	23.35	33.16
	Al_2O_3	wt.%	4.74	0.98	1.50	1.17	1.99	0.02	5.2
	Fe_2O_3	wt.%	3.08	1.35	2.00	0.56	0.00	0.55	2.86
	CaO	wt.%	8.70	9.61	49.00	37.21	8.66	5.66	13.64
	MgO	wt.%	12.03	2.46	8.50	3.41	6.11	0.36	2.9
	Na_2O	wt.%	1.49	0.33	0.40	1.96	0.15	0.91	0.88
	K_2O	wt.%	2.44	11.60	24.90	15.00	20.67	40.32	6.21
	TiO_2	wt.%	0.30	0.05	0.10	0.05	0.00	0.18	0.43
	MnO_2	wt.%	0.00	0.00	0.00	0.00	0.00	0.00	0.00
	P_2O_5	wt.%	4.31	4.20	7.80	9.37	8.68	4.01	2.49
	SO_3	wt.%	3.06	2.63	1.20	2.37	0.00	3.83	1.49
	Other	wt.%	4.21[8]	4.95	0.00	22.66	0.00	20.81[8]	30.74[8]

Footnotes:
1. The fuel and ash properties are the arithmetic mean of the values in Table S1.3;
2. The ash property is the arithmetic mean of the values in Table S1.4;
3. Fuel properties are adjusted to an as-received basis using Equation (1.1) from the values reported in Table S1.3;
4. The Carbon value is adjusted so that the total sum is 100%;
5. Hydrogen weight percentage is adjusted using Equation (1.2) from the value reported in Table S1.3;
6. Oxygen weight percentage is adjusted using Equation (1.3) from the value reported in Table S1.3;
7. The SiO_2 value is adjusted so that the total sum is 100%;
8. The Other value is adjusted so that the total sum is 100%.

1.4 Fuel Cost

The default fuel costs are estimated based on various literature using Equations (1.4) to (1.10). The costs of waste coal and biomass in IECM are expressed in the 2022 cost year. Cost adjustment is made using Equations (1.11) if the estimated cost data is in a different cost year.

Waste coal costs are derived from the Energy Information Administration (EIA) Coal Data Explorer platform (EIA, 2023). Table 1.4 presents the national- and state-level as-delivered costs for waste coal in 2021 and 2022, reported in current dollars. As waste coal samples are collected from the Illinois Basin (Kolker et al., 2021), the waste coal as-delivered costs in Illinois State are embedded into IECM.

Table 1.4. As-Delivered Waste Coal Cost.

Location	**Price (2021$/tonne)**	**Price (2022$/tonne)**
United States	16.49	18.30
Pennsylvania	15.01	18.04
West Virginia	28.92	N/A[1]
Illinois[2]	16.49	18.30

Footnotes:
1. N/A stands for Not Available;

2. For states without specific cost data, the U.S. national average cost is applied.

Biomass costs are estimated using relevant technical reports from the NETL and the International Renewable Energy Agency (IRENA). The costs for hybrid poplar, switchgrass, and torrefied wood are estimated based on the methodologies of Black et al. (2012), Buchheit et al. (2021), and Stevens et al. (2021), respectively. The costs for miscanthus, corn stover, wheat straw, and pine spruce chips are estimated using the energy-based feedstock costs reported by IRENA (2015), in conjunction with mass-based transport cost (Stolaroff et al., 2021) and assumed transport distance. In the following paragraph, we first discuss the estimation methodology for hybrid poplar, switchgrass, and torrefied wood, as outlined in Equations (1.4) to (1.7), and then introduce the estimation methodology for miscanthus, corn stover, wheat straw, and pine spruce chips in Equations (1.8) to (1.10).

The cost estimation formulas for hybrid poplar and switchgrass are shown in Equations (1.4) to (1.6), and the formula for torrefied wood is presented in Equation (1.7). In Equations (1.5) and (1.6), the default costs are estimated based on the reported biomass properties and methods (Black et al., 2012; Buchheit et al., 2021) in conjunction with the external biomass feedstock consumption rate for 20 wt.% coal-biomass co-firing power plant derived from the IECM model (2021). In Equation (1.7), the default cost is estimated based on the reported capital and O&M costs (Stevens et al., 2021) in conjunction with the assumed transport distance (64 km) and cost ($0.10/tonne-km) (Stevens et al., 2021).

$$\mathrm{F_D} = (1 - \mathrm{M}) \times \mathrm{F_{AR}} \tag{1.4}$$

$$\mathrm{ADC_{HP}} = (1.136 \times 10^{-11} \times \mathrm{F_D^3} - 2.675 \times 10^{-7} \times \mathrm{F_D^2} + 3.153 \times 10^{-3} \times \mathrm{F_D} + 116.2) \times (1 - \mathrm{M}) \times \mathrm{F^{STtMT}} \tag{1.5}$$

$$\mathrm{ADC_{SG}} = (1.286 \times 10^{-11} \times \mathrm{F_D^3} - 3.028 \times 10^{-7} \times \mathrm{F_D^2} + 3.569 \times 10^{-3} \times \mathrm{F_D} + 85.32) \times (1 - \mathrm{M}) \times \mathrm{F^{STtMT}} \tag{1.6}$$

$$\mathrm{ADC_{TW}} = \frac{\mathrm{CapC} \times \mathrm{CCF} + \mathrm{WC} + \mathrm{NGC} + \mathrm{EC} + \mathrm{OMC}}{\mathrm{PR} \times \mathrm{CF} \times 365} \times \mathrm{F^{STtMT}} + \mathrm{TC_{TW}} \tag{1.7}$$

The cost calculation formulas for miscanthus, corn stover, wheat straw, and pine spruce chips are shown in Equations (1.8) to (1.10). The costs for the biomass are estimated based on the summation of feedstock cost and transport cost, as shown in Equation (1.8). The feedstock cost includes the expense of biomass cultivation (or acquisition), harvest, and delivery to the field edge or roadside (DOE, 2011). The transport cost includes the expenses associated with picking up the biomass from the field edge or roadside and transporting it to the end users. The energy-based feedstock costs are retrieved from the IRENA report (2015) and listed in Table S1.5. These reported cost data are based on the low heating value of biomass (Table S1.5). Equations (1.9) and (1.10) are used to convert energy-based feedstock costs to mass-based feedstock costs. In Equation (1.10), the low heating value of biomass is estimated based on the higher heating value, moisture content, and hydrogen content of each biomass (EPA, 2007). The transport cost of the truck is derived from the literature and shown in Table S1.6 (Stolaroff et al., 2021). The assumed truck transport distance is 98 km (Mahmudi and Flynn, 2006; Kumar et al., 2005). The mass-based costs for the biomass are determined by multiplying the average energy-based feedstock costs by their heating value, plus the transport cost. Note that the cost summation requires all components to be in the same cost year.

$$\mathrm{ADC_m = FC_m \times F^{STtMT} + TC_m \times TD} \quad (1.8)$$
$$\mathrm{FC_m = FC_e \times LHV \times F^{MMBtu} \times F^{STtlb}} \quad (1.9)$$
$$\mathrm{LHV_{eu} = HHV_{eu} - 10.55 \times (M + 9 \times HA)} \quad (1.10)$$

Biomass costs are adjusted to 2022 dollars using the Consumer Price Index (CPI) (Bureau of Labor Statistics, 2023). The annual average chained consumer price index for all urban consumers (C-CPI-U) serves as the cost index for these adjustments, as displayed in Equation (1.11). The adjusted costs are presented in Table 1.5.

$$\mathrm{RDA = RDB \times \frac{CPIA}{CPIB}} \quad (1.11)$$

Note that the as-delivered costs for waste coal and biomass vary based on their properties, processing treatment, as well as transport method and distance. The default as-delivered costs in IECM may not be suitable for all co-firing scenarios.

Table 1.5. As-Delivered Biomass Cost.

Biomass Category	**Feedstock**	**Price (2022$/tonne)**
Energy Crop	Switchgrass	112.8
	Miscanthus	108.3
	Hybrid Poplar	100.9
	Torrefied Wood	123.6
Agricultural Residue	Corn Stover	55.9
	Wheat Straw	56.6
Forestry Residue	Pine Spruce Chips	40.9

Section 2: Boiler Efficiency Algorithm

This section consists of 3 parts: (1) “Nomenclature” shows the symbol for the parameter in formulas, (2) “Boiler Efficiency” shows the algorithm used to calculate the boiler efficiency for a power plant, and (3) “Type of Heat Loss” shows the estimation formula for each type of heat loss involved in the boiler efficiency algorithm.

2.1 Nomenclature

Symbol

C_p^{BotAsh}	specific heat of bottom ash (kJ/kg•°C)
C_p^{FlyAsh}	specific heat of fly ash (kJ/kg•°C)
C_{ash}	concentration of carbon in collected ash (fraction)
C_{co}	burned carbon as CO (fraction)
f_{ash}	as-received ash content of the fuel (mass fraction)
f_{cab}	as-received carbon content of fuel (mass fraction)
f_H	as-received hydrogen content of fuel (mass fraction)
f_{H2O}	as-received moisture content of fuel (mass fraction)
f_s	as-received sulfur content of fuel (mass fraction)
F_{ubc}	unburned carbon content in fly ash (%)
HHV_{fuel}	higher heating value of the flue on an as-received basis (kJ/kg)
$h_{H2O}(T)$	enthalpy of H_2O component in flue gas at temperature T (kJ/kg•mole)
$h_j(T)$	enthalpy of component j in flue gas at temperature T (kJ/kg•mole)
HR_{steam}	steam cycle heat rate of power plant (Btu/kWh)
HV_{cab}	heating value of the carbon, with a value of 32,797 (kJ/kg)
HV_{co}	heating value of the CO, with a value of 22,690 (kJ/kg)
L_{H2O}^{LE}	latent heat loss from water vapor (fraction)
L_{H2O}^{SE}	sensible heat loss from water vapor (fraction)
LH_{H2O}	latent heat for water vapor, with a value of 2,419 (kJ/kg)
L_{Ashes}	losses from fly ash and bottom ash (fraction)
L_{Botash}	sensible heat loss from bottom ash (fraction)
L_{Cab}	losses from unburned carbon and carbon monoxide (fraction)
L_{Flyash}	sensible heat loss from fly ash (fraction)
L_{Gas}	sensible heat loss of dry flue gas (fraction)
L_{H2O}	sensible and latent heat losses from water vapor (fraction)
L_R	loss from radiation exchange with the surroundings (fraction)
L_{Unacc}	unaccounted loss, including miscellaneous tolerance errors (fraction)
$m_{fagphi,H2O}$	kilogram moles of H_2O component in flue gas entering air preheater (kg•mole/kg_{fuel})
$m_{fagphi,j}$	kilogram moles of component j in flue gas entering air preheater (kg•mole/kg_{fuel})
M_{Botash}	mass flow rate of bottom ash exiting the bottom of the boiler (kg/hour)
M_{Flyash}	mass flow rate of fly ash exiting the boiler (kg/hour)
M_{fuel}	mass flow rate of fuel (kg/hour)
$mole_H$	molecular weight of H, with a value of 1.01 (g/mole)
$mole_{H2O}$	molecular weight of H_2O, with a value of 18.02 (g/mole)
MW_g	gross electricity output of a power plant (MW_g)

Percent	percentage of a component in the blended fuel (wt.%)
P_{flyash}	percentage of ash entering flue gas stream (%)
$S_{retained}$	sulfur retained in ash (%)
Subscript H_2O	H_2O component in combustion air and flue gas
Subscript j	components in combustion air and flue gas, including CO, CO_2, N_2, NO, NO_2, O_2, SO_2, SO_3
Subscript orig	measurement happens at the base plant where no pollution control equipment is included
Superscript bio	biomass
Superscript blend	blended fuel
Superscript c	coal
Superscript max	maximum boundary of concentration of carbon in collected ash
Superscript wc	waste coal
T_{botfu}	temperature of the bottom ash exiting the bottom of the boiler (°C)
T_{fdfan}	flue gas temperature exiting forced draft fan (°C)
T_{unc}	uncorrected flue gas temperature after the heat exchanger (°C)
VM	as-received volatile matter content of fuel (wt.%)
η_{boiler}	boiler efficiency of the power plant (fraction)

2.2 Boiler Efficiency

The boiler efficiency algorithm (η_{boiler}) in IECM (2019b) is determined using the energy balance method, which calculates net boiler efficiency by deducting heat losses to the environment, as displayed in Equation (2.1). Six heat losses are considered in this algorithm. They are the sensible heat loss of dry flue gas (L_{Gas}), sensible and latent heat losses from water vapor (L_{H2O}), losses from unburned carbon and carbon monoxide (L_{Cab}), radiation loss (L_R), losses from fly and bottom ashes (L_{Ashes}), and unaccounted loss (L_{Unacc}). After determining these six types of heat losses, the boiler efficiency of the base plant without any pollution control equipment can be calculated.

$$\eta_{boiler} = 1 - L_{Gas} - L_{H2O} - L_{Cab} - L_{Ashes} - L_R - L_{Unacc} \tag{2.1}$$

2.3 Type of Heat Loss

(a) Heat Loss from Dry Flue Gas

The sensible heat loss in dry flue gas (L_{Gas}) is the difference in heat content of dry flue gas at the uncorrected air preheater temperature and the atmospheric air temperature (IECM, 2019b). Heat loss from water vapor in flue gas is calculated separately from heat loss from dry flue gas.

$$L_{Gas} = \frac{\sum_j^8 m_{fgaphi,j,orig} \times \left(h_j\left(T_{unc,orig}\right) - h_j\left(T_{fdfan,orig}\right)\right)}{HHV_{fuel}} \tag{2.2}$$

(b) Heat Loss from Water Vapor

Heat losses due to water vapor (L_{H2O}) include latent and sensible heat losses. The latent heat loss is from the vaporization of moisture and the combustion of hydrogen in the fuel, and sensible heat loss is from water vapor in the flue gas (Singer, 1981).

$$L_{H2O} = L_{H2O}^{LE} + L_{H2O}^{SE} \tag{2.3}$$

$$L_{H2O}^{LE} = \frac{\left(f_{H2O} + \frac{mole_{H2O} \times f_H}{2 \times mole_H}\right) \times LH_{H2O}}{HHV_{fuel}} \tag{2.4}$$

$$L_{H2O}^{SE} = \frac{m_{fagphi,H2O,orig} \times \left(h_{H2O}\left(T_{unc,orig}\right) - h_{H2O}\left(T_{fdfan,orig}\right)\right)}{HHV_{fuel}} \tag{2.5}$$

(c) Heat Loss from Unburned Carbon and Carbon Monoxide

Heat loss due to incomplete oxidation (L_{Cab}) is associated with the unburned carbon (UBC) in ash and carbon monoxide (CO) in flue gas.

$$L_{Cab} = \frac{f_{cab} \times HV_{co} \times C_{co} + HV_{cab} \times f_{ash} \times \frac{C_{ash}}{1 - C_{ash}}}{HHV_{fuel}} \tag{2.6}$$

The concentration of carbon in collected ash estimation in coal and waste coal ($C_{ash}^{c,wc}$) relies on empirical data from Yilmaz (2021) and the ash distribution data from IECM (2021). Equation (2.7) presents the regression formula from Yilmaz (2021) which estimates the UBC concentration in fly ash at coal-fired power plants using the volatile matter (VM) of the coal. Equation (2.8) outlines the formula for determining the $C_{ash}^{c,wc}$, utilizing the estimated UBC in fly ash and the distribution data for the fly and bottom ashes (IECM, 2021).

$$F_{ubc}^{c,wc} = 43.927 - 1.2075 \cdot VM^{c,wc} \tag{2.7}$$

$$C_{ash}^{c,wc} = \frac{F_{ubc}^{c,wc}}{P_{flyash}} \tag{2.8}$$

The concentration of carbon in collected ash estimation in biomass (C_{ash}^{bio}) relies on laboratory experimental data from Grammelis et al. (2006). The derived regression Equation (2.9) is validated by an empirical trend.

Grammelis et al. (2006) analyzed ash samples of lignite and olive kernels co-firing cases and determined the unburned carbon concentration in ash through loss-on-ignition analysis. The empirical trend used is that for every 10% increase in biomass co-firing level on an energy basis, there is a corresponding 1% decrease in boiler efficiency (Miedema et al., 2017; Pronobis and Wojnar, 2013).

$$C_{ash}^{bio} = \frac{0.3714 \cdot VM^{bio} - 5.9865}{100} \tag{2.9}$$

The minimum C_{ash} boundary is set to 0 for all fuels. The maximum value is constrained based on the fuel properties and the concentration of post-combusted ashes, UBC, and sulfur, as shown in Equation (2.10).

$$C_{ash}^{max} = \frac{f_c}{f_c + f_{ash} + f_s \times \frac{S_{retained}}{100}} \tag{2.10}$$

The C_{ash} estimation formula for blended fuel is presented in Equation (2.11).

$$C_{ash}^{blend} = \frac{Percent^{c}}{100} \times \frac{43.927 - 1.2075 \cdot VM^{c}}{P_{flyash}} + \frac{Percent^{wc}}{100} \times \frac{43.927 - 1.2075 \cdot VM^{wc}}{P_{flyash}} + \frac{Percent^{bio}}{100} \times \frac{\left(0.3714 \cdot VM^{bio} - 5.9865\right)}{100} \quad (2.11)$$

(d) Heat Loss from Ash

Heat losses due to fly ash and bottom ash (L_{Ashes}) can be significant. Hot ashes produced by fuel combustion can lead to substantial heat losses, depending on the quantity of ash and its temperature.

$$L_{Ashes} = L_{Flyash} + L_{Botash} \quad (2.12)$$

The fly ash heat loss (L_{Flyash}) primarily stems from the fly ash carried by the flue gas leaving the boiler, representing the heat loss in the flue dust (Singer, 1981). Equation (2.13) displays the estimation formula for sensible heat loss from fly ash (Singer, 1981).

$$L_{Flyash} = \frac{M_{FlyAsh}}{M_{fuel}} \times \frac{C_{p}^{FlyAsh} \times (T_{unc} - T_{fdfan})}{HHV_{fuel}} \quad (2.13)$$

The bottom ash heat loss (L_{Botash}) comes from the bottom ash leaving the bottom of the boiler, representing the heat loss in the waste removed from the ash pit (Singer, 1981). Equation (2.14) displays the estimation formula for sensible heat loss from bottom ash.

$$L_{Botash} = \frac{M_{BotAsh}}{M_{fuel}} \times \frac{C_{p}^{BotAsh} \times (T_{botfu} - T_{fdfan})}{HHV_{fuel}} \quad (2.14)$$

The specific heat of fly ash and bottom ash are needed for the above calculations. The values are retrieved from coal combustion cases in the American Society of Mechanical Engineers (ASME) (1964), as detailed in Table 2.1.

Table 2.1 Specific Heat of Ash.

Name	**Unit**	**Value**	**Source of Data**
Specific Heat of Fly Ash	kJ/kg•°C	0.84[1]	ASME (1964)
Specific Heat of Bottom Ash	kJ/kg•°C	1.05[2]	ASME (1964)

Footnotes:
1. The value is retrieved from the 7.3.2.12 equation of ASME (1964);
2. The value is retrieved from the 7.3.2.10 equation of ASME (1964).

(e) Heat Loss from Radiation Exchange

Radiant heat loss (L_R) consists of heat lost to the surrounding air through radiation (Singer, 1981).

$$L_R = 0.0015 + \frac{600}{MW_g \times HR_{steam}} \tag{2.15}$$

(f) Unaccounted Loss

The unaccounted loss (L_{Unacc}) refers to losses that are unclassified and challenging to measure (Singer, 1981).

$$L_{Unacc} = 0.005 \tag{2.16}$$

Section 3: Life Cycle Greenhouse Gas Emission Model

This section consists of 3 parts: (1) "Nomenclature" shows the symbol for the parameter in formulas, (2) "Analysis Scope and Method" introduces the life cycle assessment boundary and the overall life cycle greenhouse gas (GHG) emission calculation formula for a power plant, and (3) "Greenhouse Gas Emissions by Stage" displays the estimation formula for each component in the overall life cycle GHG emission of the power plant.

3.1 Nomenclature

Symbol

E_{diesel}	emission intensity associated with diesel production and combustion (kg CO_2eq/kg_{diesel})
E_e	emission intensity associated with electricity consumption (kg CO_2eq/MWh)
EF_{bio}	biomass supply chain GHG emissions (kg CO_2eq/kg_{bio})
EF_c	coal supply chain GHG emissions (kg CO_2eq/kg_c)
EF_{LCA}	life cycle emissions of a power plant (kg CO_2eq/MWh_{net})
EF_{plant}	stack emissions of a power plant (kg CO_2eq/hour)
$EF_{barge}^{transport}$	transport GHG emissions of barge (kg CO_2eq/kg_{fuel}/km)
$EF_{train}^{transport}$	transport GHG emissions of train (kg CO_2eq/kg_{fuel}/km)
$EF_{truck}^{transport}$	transport GHG emissions of truck (kg CO_2eq/kg_{fuel}/km)
$EF_{T\&S}$	CO_2 transport and storage GHG emissions (kg CO_2eq/kg $CO_{2\text{-captured}}$)
EF_{wc}	waste coal supply chain GHG emissions (kg CO_2eq/kg_{wc})
FR_{bio}	biomass flow rate of a power plant (kg_{bio}/hour)
FR_c	coal flow rate of a power plant (kg_c/hour)
FR_{CO_2Cap}	captured CO_2 rate of a power plant with CCS (kg $CO_{2\text{-captured}}$/hour)
FR_{wc}	waste coal flow rate of a power plant (kg_{wc}/hour)
GWP_{CH4}^{100yr}	global warming potential value of CH_4 (kg CO_2eq)
GWP_{N2O}^{100yr}	global warming potential value of N_2O (kg CO_2eq)
MW_{net}	net electricity output of a power plant (MW_{net})

Subcategories for Coal Supply

$C_{diesel}^{extraction}$	diesel consumption of coal extraction from underground or surface mines (kg_{diesel}/kg_c)
C_{diesel}^{handle}	diesel consumption of coal handling (kg_{diesel}/kg_c)
C_{diesel}^{overbu}	diesel consumption of overburden removal at surface mine (kg_{diesel}/kg_c)
C_{diesel}^{reclam}	diesel consumption of surface mine reclamation (kg_{diesel}/kg_c)
C_e^{clean}	electricity consumption of coal cleaning (MWh/kg_c)
$C_e^{extraction}$	electricity consumption of coal extraction (MWh/kg_c)
C_e^{handle}	electricity consumption of coal handling (MWh/kg_c)
C_e^{overbu}	electricity consumption of overburden removal at surface mine (MWh/kg_c)
$C_e^{ventilation}$	electricity consumption of underground mine ventilation (MWh/kg_c)
$CMM_{CH4}^{extraction}$	coal mine methane release of underground mining (kg CH_4/kg_c)
CMM_{CH4}^{overbu}	coal mine methane release of surface mining (kg CH_4/kg_c)

D_c^{barge}	barge transport distance of coal (km)
D_c^{train}	train transport distance of coal (km)
D_c^{truck}	truck transport distance of coal (km)
$EF_{clean}^{process}$	emissions of coal cleaning (kg CO_2eq/kg$_c$)
EF_c^{mining}	emissions of coal mining (kg CO_2eq/kg$_c$)
$EF_c^{process}$	emissions of coal processing (kg CO_2eq/kg$_c$)
$EF_c^{transport}$	emissions of coal transport (kg CO_2eq/kg$_c$)
$EF_{handle}^{process}$	emissions of coal handling (kg CO_2eq/kg$_c$)
EF_{sur}^{mining}	emissions of surface mining (kg CO_2eq/kg$_c$)
EF_{ung}^{mining}	emissions of underground mining (kg CO_2eq/kg$_c$)
$Em_{constru}^{clean}$	emissions of coal preparation facility construction (kg CO_2eq/kg$_c$)
$Em_{constru}^{mining}$	emissions of coal mine commission, decommission, and construction (kg CO_2eq/kg$_c$)
Em^{NH4NO3}	emissions of the ammonium nitrate fuel oil explosives consumption in surface coal extraction and overburden removal (kg CO_2eq/kg$_c$)
$loss_c^{process}$	loss factor of coal cleaning (fraction)
Subscript c	coal

Subcategories for Waste Coal Supply

$C_{diesel}^{extraction}$	diesel consumption of waste coal extraction (kg$_{diesel}$/kg$_{wc}$)
C_e^{cur}	electricity consumption of waste coal cold-curing (MWh/kg$_{wc}$)
C_e^{dens}	electricity consumption of waste coal densification (MWh/kg$_{wc}$)
C_e^{wash}	electricity consumption of waste coal washing (MWh/kg$_{wc}$)
D_{wc}^{barge}	barge transport distance of waste coal (km)
D_{wc}^{train}	train transport distance of waste coal (km)
D_{wc}^{truck}	truck transport distance of waste coal (km)
$EF_{wc}^{extraction}$	emissions of waste coal extraction (kg CO_2eq/kg$_{wc}$)
$EF_{wc}^{process}$	emissions of waste coal processing (kg CO_2eq/kg$_{wc}$)
$EF_{wc}^{transport}$	emissions of waste coal transport (kg CO_2eq/kg$_{wc}$)
$F^{m3tliter}$	unit conversion between cubic meter and liter, with a value of 1000 (L/m^3)
$F^{litertkg}$	unit conversion between liter and kg, with a value of 0.84 (kg/liter)
$loss_{wc}^{extracted}$	loss factor of extracted waste coal to waste coal product (kg$_{extracted}$/kg$_{wc}$)
$loss_{wc}^{pellets}$	loss factor of waste coal pellet to waste coal product (kg$_{pellet}$/kg$_{wc}$)
$loss_{wc}^{slurry}$	loss factor of coal-rich slurry (kg$_{slurry}$/kg$_{wc}$)
Subscript wc	waste coal

Subcategories for Biomass Supply

$\frac{44}{12}$	molecular weight conversion factor from C to CO_2 (fraction)
AC^{soil}	annual carbon stored in soil (kg C/hectare$_{bio}$/year)
$Area_H$	tree harvester covered area per unit time (hectare/hour)
BW	baler width (feet)
$C^{abovegnd}$	carbon fraction of aboveground biomass (kg C/kg$_{bio}$)

$C_{oth}^{abovegnd}$ carbon fraction of dry aboveground biomass for other land (kg C/hectare$_{bio}$)
C^{root} carbon stored in biomass root (kg C/hectare$_{bio}$)
C^{soil} carbon stored in soil (kg C/hectare$_{bio}$)
$CO_2^{abovegnd}$ carbon dioxide equivalent emissions from aboveground biomass (kg CO_2eq/kg$_{bio}$)
$CO_2^{belowgnd}$ carbon dioxide equivalent emissions from belowground biomass (kg CO_2eq/kg$_{bio}$)
CO_2^{soil} carbon dioxide equivalent emissions from soil (kg CO_2eq/kg$_{bio}$)
D_{bio}^{barge} barge transport distance of biomass (km)
D_{bio}^{train} train transport distance of biomass (km)
D_{bio}^{truck} truck transport distance of biomass (km)
DS speed of tractor when dragging the disk tiller (mile/hour)
DT number of disk tiller pass needed before a planting (#)
DW disk tiller width (feet)
E_{CH4} CH_4 release per biomass input to the torrefaction (kg CH_4/kg$_{bio-in}$)
E_{CO2} CO_2 release per biomass input to the torrefaction (kg CO_2/kg$_{bio-in}$)
$E_{herbicide}$ emission intensity associated with herbicide consumption (kg CO_2eq/kg$_{herbicide}$)
E_{N2O} N_2O release per biomass input to the torrefaction (kg N_2O/kg$_{bio-in}$)
fb fraction of biomass yield assumed to be present when estimating biomass carbon stocks (fraction)
FC fuel consumption for harvester (lb$_{diesel}$/hp/hour)
F^{MJtMWh} unit conversion between MJ and MWh, with a value of 1/3600 (MWh/MJ)
F^{hatft2} unit conversion between hectare and square feet, with a value of 107,639 (ft^2/hectare)
$F^{gatliter}$ unit conversion between gallon and liter, with a value of 3.79 (liter/gallon)
$F^{lbtliter}$ unit conversion between pound and liter for diesel, with a value of 0.5391 (liter/lb)
$F^{litertkg}$ unit conversion between liter and kg, with a value of 0.84 (kg/liter)
$F^{miletft}$ unit conversion between mile and feet, with a value of 5,280 (feet/mile)
F_{oth2cr} cropland created from other land due to indirect land use change (fraction)
$EF_{bio}^{cultivation}$ biomass cultivation emissions (kg CO_2eq/kg$_{bio}$)
EF_{bio}^{dluc} direct land use change emissions (kg CO_2eq/kg$_{bio}$)
EF_{bio}^{grind} emissions of biomass grinding (kg CO_2eq/kg$_{bio}$)
$EF_{bio}^{harvest}$ emissions of biomass harvesting (kg CO_2eq/kg$_{bio}$)
EF_{bio}^{iluc} indirect land use change emissions (kg CO_2eq/kg$_{bio}$)
EF_{bio}^{luc} direct and indirect land use change emissions (kg CO_2eq/kg$_{bio}$)
$EF_{bio}^{process}$ emissions of biomass processing (kg CO_2eq/kg$_{bio}$)
$EF_{bio}^{production}$ biomass production emissions (kg CO_2eq/kg$_{bio}$)
EF_{bio}^{torref} emissions of biomass torrefaction (kg CO_2eq/kg$_{bio}$)
$EF_{bio}^{transport}$ emissions of biomass transport (kg CO_2eq/kg$_{bio}$)
$EF_{dsluse}^{cultivation}$ emissions associated with diesel consumption during biomass cultivation (kg CO_2eq/kg$_{bio}$)

$EF_{fertuse}^{cultivation}$	emissions associated with fertilizer consumption during biomass cultivation (kg CO_2eq/kg_{bio})
$EF_{herbuse}^{cultivation}$	emissions associated with herbicide consumption during biomass cultivation (kg CO_2eq/kg_{bio})
$EFactor_{allo}$	energy-based emission allocation factor
FU	manufacturer fuel use at standard power take-off at 1953 rpm tractor which is used for dragging the disk tiller and planter (gallon/hour)
FUT	manufacturer fuel use of tractor and baler (gallon/hour)
GC	planting increment cycle of biomass (year)
HD	header operating speed of harvester (mile/hour)
HHV	higher heating value (kJ/kg)
HI	harvest index. It represents the grain yield of a crop as a fraction of aboveground biomass production, indicating the distribution of production between grain and agricultural residue (fraction)
HPE	horsepower for harvester (hp)
HWH	header width of the harvester (feet)
$loss_{bio}^{gnd}$	loss factor of biomass grinding (fraction)
$loss_{bio}^{tor}$	loss factor of biomass torrefaction (fraction)
mf_c	carbon content of biomass (mass fraction)
mf_{H2O}	moisture content of biomass (mass fraction)
$mole_N$	molecular weight of N, with a value of 14 (g/mole)
$mole_o$	molecular weight of O, with a value of 16 (g/mole)
$N2O_{soil}^{dir}$	N_2O emission as the land changed to biofuel production from displaced cropland (kg N_2O/kg_{bio})
$N2O_{soil}^{ind}$	N_2O emission from indirectly created cropland (kg N_2O/kg_{bio})
N	amount of nitrogen fertilizer consumed (kg N/hectare/year)
NV_N	ratio of non-volatilized fertilizer to total nitrogen fertilizer (fraction)
NV_{N2O}	ratio of N_2O release from soil (fraction)
p	efficiency of agricultural residue collection from cropland (fraction)
PS	speed of tractor when dragging the planter (mile/hour)
PT	number of planter pass needed during planting (#)
PW	planter width (feet)
$ratio_c$	ratio of as-received carbon content of raw willow to torrefied willow (fraction)
$ratio_{ILUC/DLUC}$	fraction of a hectare of indirect land use change in a remote area, resulting from the conversion of one hectare in direct land use change (fraction)
$ratio_{R2S}$	root-to-shoot ratio of the plant (fraction)
$ratio_{residue}$	ratio of harvest residues to yield (fraction)
$ratio_{usel}$	electricity consumption ratio of torrefaction process to grinding process (fraction)
rN_2O	volatilized N_2O per unit of nitrogen fertilizer (kg N_2O/kg N)
S	share of land (fraction)
Subscript bio	biofuel production
Subscript biofcr	land changed to biofuel production from cropland
Subscript biofpa	land changed to biofuel production from pastureland
Subscript cr	cropland

Subscript crfoth	land changed to cropland from other land
Subscript crfpa	land changed to cropland from pastureland
Subscript ec	energy crop
Subscript fr	forestry residue
Subscript hp	herbaceous product
Subscript hr	herbaceous residue
Subscript oth	other land, consisting of both high and low carbon-stock areas, holds an average carbon stock of approximately half of the typical values found in temperate zone forests
Subscript pa	pastureland
Subscript pafoth	land changed to pastureland from other land
Subscript pr	agricultural product
Subscript re	agricultural residue
Subscript TW	torrefied wood
Subscript wp	woody product
Subscript wr	woody residue
Superscript dry	dry basis
Superscript G	pre-harvested
Superscript wet	wet basis
T	study period, with a value of 30 (year)
Tb	period for estimating biomass carbon stock (year)
TO	tractor operating speed (mile/hour)
$Uptake_{CO2}$	CO_2 uptake during the biomass growth (kg CO_2/kg_{bio})
U_{dc}	diesel consumption during biomass cultivation (kg_{diesel}/hectare/year)
U_{dh}	diesel consumption during biomass harvesting (kg_{diesel}/kg_{bio})
U_e	electricity consumption during biomass grinding (MJ/kg_{bio})
U_h	herbicide consumption during biomass cultivation ($kg_{herbicide}$/hectare/year)
V_N	ratio of volatilized fertilizer to total nitrogen fertilizer (fraction)
V_{N2O}	nitrogen fertilizer volatilizes nitrogen to form N_2O (fraction)
Y	annual biomass yield (kg/hectare/year)
Z	annual biomass yield (short-ton/acre/year)

Subcategories for CO_2 Transport and Storage

$Area_{survey}$	seismic survey area (km^2/kg $CO_{2\text{-captured}}$)
C_{diesel}^{consSt}	diesel consumption of well installation (kg_{diesel}/well)
$C_{diesel}^{storage}$	diesel consumption of 3D Seismic-site preparation & site monitoring survey operation (kg_{diesel}/km^2)
$C_e^{storage}$	electricity consumption of site operations & brine management (MWh/kg $CO_{2\text{-captured}}$)
$Deliver_{CO2}$	daily CO_2 delivery amount (tonne/day)
$Density_{CO2}$	CO_2 gas density at standard temperature and pressure, namely 32°F and 14.5 psi (kg/m^3)
$Density_{pipeline}$	density of steel pipeline (kg/mile)
D_{pipe}	pipeline diameter (inch)
$Drill_{depth}$	well depth (m/well)
$Drill_{power}$	power of drilling equipment (MW)

$Drill_{speed}$	drilling rate of the well (m/h)
$E^{Transport}_{construction}$	emissions associated with the construction of CO_2 transport pipeline (kg CO_2eq/kg $CO_{2\text{-captured}}$)
$E^{Transport}_{pig}$	emissions associated with the pigging operation of CO_2 transport pipeline (kg CO_2/kg $CO_{2\text{-captured}}$)
$E^{Transport}_{pumpleak}$	emissions associated with leakage of the CO_2 injection pump of CO_2 transport pipeline (kg CO_2/kg $CO_{2\text{-captured}}$)
$E^{Transport}_{fugitive}$	emissions associated with the fugitive of CO_2 transport pipeline (kg CO_2/kg $CO_{2\text{-captured}}$)
$E^{storage}_{formleak}$	geological formation storage leakage (kg CO_2eq/kg $CO_{2\text{-captured}}$)
$E^{storage}_{wellconstruction}$	emissions associated with the construction of injection well (kg CO_2eq/kg $CO_{2\text{-captured}}$)
$E^{storage}_{suvery}$	emissions associated with 3D Seismic-site preparation & site monitoring survey operation (kg CO_2eq/kg $CO_{2\text{-captured}}$)
$E^{constru}_{GHG}$	emissions of the well construction (kg CO_2eq/well)
E_{pump}	emissions for CO_2 released to air from CO_2 pump (kg/MW-day)
E_{steel}	emission intensity associated with steel production (kg CO_2eq/kg_{steel})
$E_{survery}$	emissions per seismic survey area (kg CO_2eq/km^2)
$EF^{Transport}_{CO2}$	CO_2 transport GHG emissions (kg CO_2eq/kg $CO_{2\text{-captured}}$)
$EF^{Storage}_{CO2}$	CO_2 storage GHG emissions (kg CO_2eq/kg $CO_{2\text{-captured}}$)
$Fugiative_{CH4}$	methane fugitive emission of natural gas pipeline (m^3/km-yr)
F^{kmtmi}	unit conversion between kilometer and mile, with a value of 0.62 (mile/km)
F^{yrtdy}	unit conversion between year and day, with a value of 365.25 (day/year)
F^{kgtMT}	unit conversion between kg and tonne, with a value of 10^{-3} (tonne/kg)
$Leak_{CO2}$	CO_2 leak factor of pipeline (unitless)
L_{pipe}	CO_2 pipeline length (mile)
Num_{well}	number of well required (#)
$Period_{pipe}$	study period for the CO_2 pipeline and injection (years)
$Power_{pump}$	power requirements for CO_2 pump (MW)
$Steel_{well}$	amount of pipe welded steel required per well (kg_{steel}/well)
$Tortuosity_{pipe}$	pipeline tortuosity factor (unitless)
U_d	diesel consumption per unit of brake specific drilling energy (kg_{diesel}/MWh)
$weight_{pipe}$	additional pipeline weight factor due to valves (unitless)

3.2 Analysis Scope and Method

The boundary of the life cycle assessment (LCA) is shown in Figure 3.1. The major life cycle stages for electricity generation plants include fuel supply, combustion-based power generation, and, when applicable, CO_2 transport and storage. Depending on the plant type, fuel may include coal, waste coal, and biomass, which have different supply chains. The coal supply chain involves mining, processing, and transport. The waste coal supply chain consists of extraction, processing, and transport. The biomass supply chain includes land use change, production, harvesting and handling, processing, and transport. The combustion-based power generation consists of the base plant, pollution control systems, and the amine-based post-combustion carbon capture when applicable. The CO_2 transport and storage covers pipeline transport and geological sequestration.

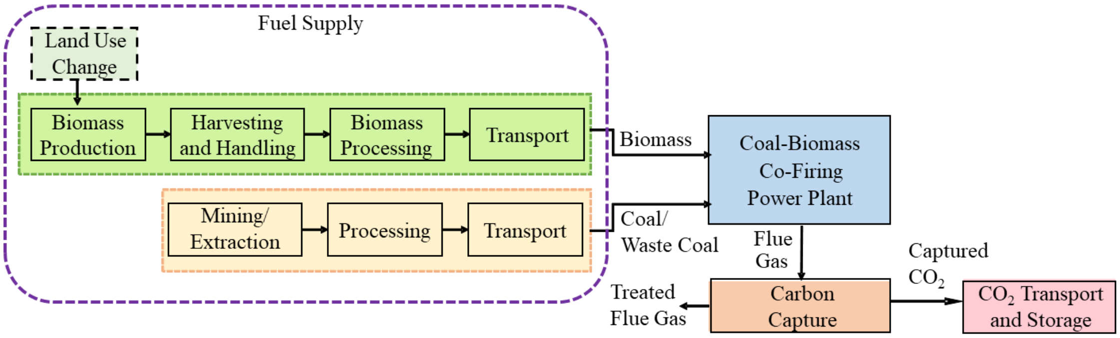

Figure 3.1. Life Cycle Boundary of Co-Firing Power Plant with Carbon Capture and Storage.

Based on the scope of the LCA, a fuel-based life cycle GHG model is developed. This model is integrated into the IECM. The IECM can then be used to perform a process-based LCA. The functional unit of LCA is 1 MWh of electricity delivered to the power grid. The life cycle emissions of the power plants are estimated using Equation (3.1), based on the IECM modeling results and each stage's GHG emissions. The GHG emission estimation method for each stage is presented below. The considered GHG include CO_2, CH_4, and N_2O, with their Global Warming Potential (GWP) values reported in Table S2.1 (IPCC, 2014).

GHG Emissions of Co-Firing Power Plants

$$EF_{LCA} = EF_c \times \frac{FR_c}{MW_{net}} + EF_{wc} \times \frac{FR_{wc}}{MW_{net}} + EF_{bio} \times \frac{FR_{bio}}{MW_{net}} + \frac{EF_{plant}}{MW_{net}} + EF_{T\&S} \times \frac{FR_{CO_2Cap}}{MW_{net}} \quad (3.1)$$

3.3 Greenhouse Gas Emissions by Stage

This subsection introduces and summarizes the GHG emissions estimation method by stage. It begins with the stage of fuel supply, followed by electricity generation plant operation and CO_2 transport and storage.

(a) Fuel Supply

The fuels of interest include coal, waste coal, and biomass. For each, we present a brief introduction, calculation formulas, emission results, and discussions.

Coal Supply

Coal is extracted through surface or underground mining, and then processed as needed before being transported to the power plant by train, truck, or barge. The coal supply chain emissions are calculated in Equation (3.2). Energy consumption and associated GHG emissions of the coal supply chain are estimated based on NETL unit process files (NETL, 2009, 2010, 2011, 2013a–2013e), NETL technical reports (Skone et al., 2016; Cutshaw et al., 2023), and the NETL CO_2U LCA guidance toolkit (NETL, 2023). The calculation details for coal supply emissions are listed in Equations (3.3) to (3.10). Table 3.1 summarizes the input for the coal supply chain GHG emissions calculation. Table 3.2 summarizes the emissions of coal supply chain for Illinois No. 6 Coal and Powder River Basin Coal.

Coal Mining. This study considers coal samples from different mining approaches. For underground mining, GHG emissions come from several sources, including mine commission, construction, coal extraction, underground gas ventilation, and decommission (Cutshaw et al., 2023). For surface mining, GHG emissions are associated with mine commission, construction, overburden removal, coal extraction, mine reclamation, and decommission (Cutshaw et al., 2023).

Coal Processing. GHG emissions of coal processing result from activities such as coal handling and cleaning, which vary based on the coal type and processing requirements (Cutshaw et al., 2023). Coal processing includes the energy needed to transport coal around the mine site using trucks, conveyor belts, load-haul-dump machines, bulldozers, and front-end loaders (Cutshaw et al., 2023). Coal cleaning involves processes on the mine site to separate coal from rocks, dirt, clay, and other materials (Cutshaw et al., 2023).

Coal Transport. The emissions for each transport method (kg CO_2eq/kg_{fuel}/km) are derived from literature (NETL, 2010, 2011; Federal LCA Commons, 2020). The transport GHG emissions can be affected by vehicle type, geography, equipment efficiency, upstream fuel production emission, and climate conditions (Facanha and Horvath, 2007; O'Connell et al., 2023). The transport GHG emissions (kg CO_2eq/kg_{fuel}) vary based on the vehicle fuel consumption rate and carrying capacity as well as the transport distance of the fuel location and the power plant.

GHG Emissions of Coal Supply Chain

$$\mathrm{EF_c = EF_c^{mining} + EF_c^{process} + EF_c^{transport}} \tag{3.2}$$

GHG Emissions of Coal Mining

$$\mathrm{EF_c^{mining}} = \begin{cases} \mathrm{EF_{ung}^{mining}} \\ \mathrm{EF_{sur}^{mining}} \end{cases} \tag{3.3}$$

$$\mathrm{EF_{ung}^{mining}} = \Big(\big(\mathrm{C_e^{extraction} + C_e^{ventilation}}\big) \times \mathrm{E_e} + \mathrm{C_{diesel}^{extraction}} \times \mathrm{E_{diesel}} + \mathrm{CMM_{CH4}^{extraction}} \times \mathrm{GWP_{CH4}^{100yr}}\Big) \times \big(1 + \mathrm{loss_c^{process}}\big) + \mathrm{Em_{constru}^{mining}} \tag{3.4}$$

$$\mathrm{EF_{sur}^{mining}} = \Big(\big(\mathrm{C_e^{extraction} + C_e^{overbu}}\big) \times \mathrm{E_e} + \big(\mathrm{C_{diesel}^{extraction} + C_{diesel}^{overbu} + C_{diesel}^{reclam}}\big) \times \mathrm{E_{diesel}} + \mathrm{CMM_{CH4}^{overbu}} \times \mathrm{GWP_{CH4}^{100yr}} + \mathrm{Em^{NH4NO3}}\Big) \times \big(1 + \mathrm{loss_c^{process}}\big) + \mathrm{Em_{constru}^{mining}} \tag{3.5}$$

GHG Emissions of Coal Processing

$$\mathrm{EF_c^{process} = EF_{handle}^{process} + EF_{clean}^{process}} \tag{3.7}$$

$$\mathrm{EF_{handle}^{process}} = \big(\mathrm{C_e^{handle}} \times \mathrm{E_e} + \mathrm{C_{diesel}^{handle}} \times \mathrm{E_{diesel}}\big) \times \big(1 + \mathrm{loss_c^{process}}\big) \tag{3.8}$$

$$\mathrm{EF_{clean}^{process}} = \mathrm{C_e^{clean}} \times \mathrm{E_e} + \mathrm{Em_{constru}^{clean}} \tag{3.9}$$

GHG Emissions of Coal Transport

$$\mathrm{EF_c^{transport}} = \mathrm{EF_{train}^{transport}} \times \mathrm{D_c^{train}} + \mathrm{EF_{truck}^{transport}} \times \mathrm{D_c^{truck}} + \mathrm{EF_{barge}^{transport}} \times \mathrm{D_c^{barge}} \quad (3.10)$$

Table 3.1. Inputs of Coal Mining and Processing Emission Estimation.

Fuel Type	**Stage**	**Symbol**	**Value**	**Unit**	**Source of Data**
Illinois No. 6	Underground Mining[1]	$C_e^{extraction}$	1.8E-05	MWh/kg_c	Cutshaw et al. (2023)
		$C_e^{ventilation}$	4.3E-05	MWh/kg_c	NETL (2013a)
		$C_{diesel}^{extraction}$	4.3E-04	kg_{diesel}/kg_c	Cutshaw et al. (2023)
		$CMM_{CH4}^{extraction}$	2.7E-03	$kg\ CH_4/kg_c$	Cutshaw et al. (2023)
		$Em_{constru}^{mining}$	8.92E-04	$kg\ CO_2eq/kg_c$	Cutshaw et al. (2023)
	Underground Coal Processing[1]	C_e^{handle}	2.0E-05	MWh/kg_c	NETL (2013b)
		C_{diesel}^{handle}	1.5E-03	kg_{diesel}/kg_c	NETL (2013b)
		C_e^{clean}	4.2E-07	MWh/kg_c	NETL (2013c)
		$loss_c^{process}$	0.30	fraction	NETL (2013c), Cutshaw et al. (2023)
		$Em_{constru}^{clean}$	2.62E-05	$kg\ CO_2eq/kg_c$	Cutshaw et al. (2023)
Powder River Basin	Surface Mining[1]	C_e^{overbu}	8.6E-06	MWh/kg_c	NETL (2013d)
		$C_e^{extraction}$	7.5E-07	MWh/kg_c	NETL (2013d)
		$C_{diesel}^{extraction}$	1.6E-04	kg_{diesel}/kg_c	NETL (2013d)
		C_{diesel}^{overbu}	6.8E-04	kg_{diesel}/kg_c	NETL (2013d)
		C_{diesel}^{reclam}	1.0E-04	kg_{diesel}/kg_c	NETL (2013d)
		CMM_{CH4}^{overbu}	6.3E-04	$kg\ CH_4/kg_c$	Cutshaw et al. (2023)
		Em^{NH4NO3}	3.3E-03	$kg\ CO_2eq/kg_c$	Skone et al. (2016)
		$Em_{constru}^{mining}$	2.3E-04	$kg\ CO_2eq/kg_c$	Skone et al. (2016)
	Surface Coal Processing[1]	C_{diesel}^{handle}	1.4E-03	kg_{diesel}/kg_c	NETL (2013e)
		$loss_c^{process}$	0	fraction	Cutshaw et al. (2023)

Footnote:
1. The emission intensities associated with electricity (E_e) and diesel consumption (E_{diesel}) are displayed in Tables S2.2 and S2.3, respectively.

Table 3.2. Coal Supply Chain Emissions.

Stage / **Name**	**Illinois No. 6**	**Powder River Basin**
Mining ($kg\ CO_2eq/kg_c$)	1.7E-01	3.5E-02
Processing ($kg\ CO_2eq/kg_c$)	2.5E-02	5.5E-03
Transport ($kg\ CO_2eq/kg_c/km$)		
By Train	2.0E-05	
By Truck	1.2E-04	
By Barge	2.7E-05	

Coal mine methane (CMM) released from ventilation or overburden removal occupies a large portion of the total coal supply chain GHG emissions (Skone et al., 2016, 2018a). Factors such as coal seam depth, coal rank, and mining method are crucial in determining methane release during mining (Irving and Tailakov, 2000). Methane emissions from underground mining are typically higher than surface mining due to the greater gas content in deeper coal seams (Irving and Tailakov, 2000).

Waste Coal Supply

Waste coal is extracted from impoundments, processed, and then transported to the power plant by train, truck, or barge. The waste coal supply chain emissions are calculated in Equation (3.11). GHG emissions for each stage of the waste coal supply chain are estimated based on the energy consumption amount (Hanak, 2022) and emission intensity associated with consumption (NETL, 2011a, 2014, 2023). The calculation details for waste coal supply emissions are listed in Equations (3.12) to (3.14). Table 3.3 summarizes the input for the waste coal supply chain GHG emissions calculation. Table 3.4 summarizes the emissions of waste coal supply chain.

Waste Coal Extraction. GHG emissions are contributed by diesel-driven equipment, including a pit front-end loader, two pit trucks, and a plant front-end loader used to extract coal-rich slurry from the impoundment (Hanak, 2022).

Waste Coal Processing. GHG emissions result from electricity-powered equipment used for moisture separation, densification, and cold curing (Hanak, 2022).

Waste Coal Transport. Transport GHG Emissions (kg CO_2eq/kg$_{wc}$/km) for waste coal are assumed to be the same as those for coal transport.

GHG Emissions of Waste Coal Supply Chain

$$\mathrm{EF_{wc}} = \mathrm{EF_{wc}^{extraction}} + \mathrm{EF_{wc}^{process}} + \mathrm{EF_{wc}^{transport}} \tag{3.11}$$

GHG Emissions of Waste Coal Extraction

$$\mathrm{EF_{wc}^{extraction}} = \mathrm{C_{diesel}^{extraction}} \times \mathrm{F^{m3tliter}} \times \mathrm{F^{litertkg}} \times \mathrm{E_{diesel}} \times \left(1 + \mathrm{loss_{wc}^{slurry}}\right) \tag{3.12}$$

GHG Emissions of Waste Coal Processing

$$\mathrm{EF_{wc}^{process}} = \left(\mathrm{C_{e}^{wash}} \times \left(1 + \mathrm{loss_{wc}^{extracted}}\right) + \mathrm{C_{e}^{dens}} \times \left(1 + \mathrm{loss_{wc}^{pellets}}\right) + \mathrm{C_{e}^{cur}}\right) \times \mathrm{E_e} \tag{3.13}$$

GHG Emissions of Waste Coal Transport

$$\mathrm{EF_{wc}^{transport}} = \mathrm{EF_{train}^{transport}} \times \mathrm{D_{wc}^{train}} + \mathrm{EF_{truck}^{transport}} \times \mathrm{D_{wc}^{truck}} + \mathrm{EF_{barge}^{transport}} \times \mathrm{D_{wc}^{barge}} \tag{3.14}$$

Table 3.3. Inputs of Waste Coal Extraction and Processing Emission Estimation.

Fuel Type	Stage	Symbol	Value	Unit	Source of Data
Waste Coal	Extraction[1]	$C_{diesel}^{extraction}$	4.2E-07	m^3/kg_{slurry}	Hanak (2022)
		$Loss_{wc}^{slurry}$	4	kg_{slurry}/kg_{wc}	
	Processing[1]	C_e^{wash}	8.1E-06	$MWh/kg_{extracted}$	
		C_e^{dens}	2.3E-05	$MWh/kg_{pellets}$	
		C_e^{cur}	2.4E-06	MWh/kg_{wc}	
		$loss_{wc}^{extracted}$	0.25	$kg_{extracted}/kg_{wc}$	
		$loss_{wc}^{pellets}$	0.25	kg_{pellet}/kg_{wc}	

Footnote:
1. The emission intensities associated with electricity (E_e) and diesel consumption (E_{diesel}) are displayed in Tables S2.2 and S2.3, respectively.

Table 3.4. Waste Coal Supply Chain Emissions.

Stage \ Name	Waste Coal
Mining (kg CO_2eq/kg_{wc})	6.9E-03
Processing (kg CO_2eq/kg_{wc})	2.4E-02
Transport (kg CO_2eq/kg_{wc}/km)	
By Train	2.0E-05
By Truck	1.2E-04
By Barge	2.7E-05

The processing steps required for waste coal result in high energy consumption and GHG emissions. Waste coal processing is the primary contributor to supply GHG emissions, primarily due to the electricity used by the processing equipment.

Biomass Supply

Biomass is produced from cultivation and harvesting, processed as needed, and then transported to the power plant by train, truck, or barge. The biomass supply chain emissions are calculated in Equation (3.15). The GHG emissions of the biomass supply chain are estimated based on the methods from NETL technical reports and unit process files (Skone et al., 2011; NETL, 2010a–2010e, 2011b, 2012a–2012d, 2023) and external data of material and energy consumption rate as well as yield (Kahle et al., 2001; Jacobson et al., 2013, 2014; Song et al., 2016; Dumortier, 2018; Mann et al., 2013; Fortier et al., 2015; Caslin et al., 2015a, 2015b; USDA, 2023). The calculation details for biomass supply emissions are listed in Equations (3.16) to (3.63). Tables 3.5 to 3.9 summarize the input for the GHG emissions calculation of direct land use change, indirect land use change, CO_2 uptake, biomass cultivation, biomass harvesting, and biomass processing, respectively. Table 3.10 summarizes the emissions of the biomass supply chain for seven biomass samples.

Land Use Change. Land use change emissions associated with biomass cultivation consider both direct and indirect land use change emissions, as detailed in Equation (3.16). These emissions stem from four main components: changes in aboveground biomass, belowground biomass, soil organic matter, and fertilizer usage. These are outlined in Equations (3.17) through

(3.46). Direct land use change occurs when land previously used for other purposes is converted to biofuel production. Indirect land use change occurs when grasslands and forests are converted to cropland/pastureland somewhere on the globe to compensate for the displacement of commodities due to biofuel production (Plevin et al., 2010). Three key assumptions are made: (1) the biofuel production occurs on land that is assumed to consist of 24% cropland and 76% pastureland. This assumption follows that of Skone et al. (2011), with the reference location being Northern Missouri, (2) converting 1 hectare of land directly leads to 0.3 hectares of indirect land use change in a remote area. The ratios for direct and indirect land use change are estimated based on 2021 international land conversion data (EPA, 2010), and (3) agricultural and forestry residues are treated as waste and thus do not cause land use change.

Biomass Production. The biomass production emissions are the summation of CO_2 uptake and biomass cultivation, as shown in Equation (3.47). CO_2 uptake is calculated based on the carbon content of biomass, representing the carbon sequestered through photosynthesis during cultivation. For energy crops and forestry residues, the CO_2 uptake is estimated using Equation (3.48), and agricultural residues' CO_2 uptake is estimated using Equation (3.51). In biomass cultivation, associated GHG emissions result from energy consumption and the use of fertilizers and herbicides. The cultivation process can yield one type or multiple types of biomass. When multiple products are yielded, GHG emissions from production need proportional allocation between products. An energy-based factor, derived from the higher heating value and yield rate of each product, can be used for this allocation. Three key assumptions are made: (1) the energy crop cultivation process produces only one type of biomass, thus, no allocation is needed, (2) an energy-based allocation factor is used to allocate production GHG emissions between agricultural residue and product, and (3) no fuel/fertilizer/herbicide-consumption emissions are accounted for during the cultivation of forestry residues (Skone et al., 2012) and so no allocation factor is applied to their GHG emissions.

Biomass Harvesting. Biomass harvesting generates GHG emissions primarily from the energy consumed by harvesting equipment, as shown in Equations (3.58) to (3.59). Different types of biomass require various harvesting methods. Different harvesting methods are considered for three biomass groups: (1) herbaceous product, such as switchgrass and miscanthus, (2) herbaceous residue, such as corn stover and wheat straw, and (3) woody product and residue, such as hybrid poplar, willow, and pine spruce chips. The corresponding diesel use estimation equations are provided in Equations (3.59a) to (3.59c). Table 3.8 shows the input for estimating GHG emissions for each harvesting method.

Biomass Processing. GHG emissions of biomass processing depend on the specific processing requirements. For the biomass discussed in this report, the processes of interest include grinding and torrefaction. Grinding reduces the biomass size before it is delivered to the boiler, while torrefaction is a pretreatment process that decreases moisture and volatile matter, thereby increasing the biomass's heating value (Kopczyński et al., 2017). Studies found that co-firing torrefied biomass at a power plant achieved similar boiler efficiency to coal (Mun et al., 2016).

Biomass Transport. Transport emissions (kg CO_2eq/kg$_{bio}$/km) are assumed to be like those for coal transport.

GHG Emissions of Biomass Supply Chain

$$\mathrm{EF_{bio}} = \mathrm{EF_{bio}^{luc}} + \mathrm{EF_{bio}^{production}} + \mathrm{EF_{bio}^{harvest}} + \mathrm{EF_{bio}^{process}} + \mathrm{EF_{bio}^{transport}} \quad (3.15)$$

GHG Emissions of Land Use Change

$$EF_{bio}^{luc} = EF_{bio}^{dluc} + EF_{bio}^{iluc} \tag{3.16}$$

Direct Land Use Change

$$S_{pa} = 1 - S_{cr} \tag{3.17}$$

$$EF_{bio}^{dluc} = \left(S_{cr} \times \left(CO_{2biofcr}^{abovegnd} + CO_{2biofcr}^{belowgnd} + CO_{2biofcr}^{soil}\right) + S_{pa} \times \left(CO_{2biofpa}^{abovegnd} + CO_{2biofpa}^{belowgnd} + CO_{2biofpa}^{soil}\right) + N2O_{soil}^{dir}\right) \times \left(1 + loss_{bio}^{gnd}\right) \times (1 + loss_{bio}^{tor}) \times (1 - mf_{H2O}^{wet}) \tag{3.18}$$

$$CO_{2biofcr}^{abovegnd} = \frac{44}{12} \times \frac{-\left[\left(fb \times Tb \times Y_{bio}^{dry,G} \times C_{bio}^{abovegnd}\right) - \left(fb \times Tb \times Y_{cr}^{dry,G} \times C_{cr}^{abovegnd}\right)\right]}{Y_{bio}^{dry} \times T} \tag{3.19}$$

$$CO_{2biofpa}^{abovegnd} = \frac{44}{12} \times \frac{-\left[\left(fb \times Tb \times Y_{bio}^{dry,G} \times C_{bio}^{abovegnd}\right) - \left(fb \times Tb \times Y_{pa}^{dry,G} \times C_{pa}^{abovegnd}\right)\right]}{Y_{bio}^{dry} \times T} \tag{3.20}$$

$$CO_{2biofcr}^{belowgnd} = \frac{44}{12} \times \frac{-(C_{bio}^{root} - C_{cr}^{root})}{Y_{bio}^{dry} \times T} \tag{3.21}$$

$$CO_{2biofpa}^{belowgnd} = \frac{44}{12} \times \frac{-(C_{bio}^{root} - C_{pa}^{root})}{Y_{bio}^{dry} \times T} \tag{3.22}$$

$$CO_{2biofcr}^{soil} = \frac{44}{12} \times \frac{-C_{biofcr}^{soil}}{Y_{bio}^{dry} \times T} \tag{3.23}$$

$$CO_{2biofpa}^{soil} = \frac{44}{12} \times \frac{-C_{biofpa}^{soil}}{Y_{bio}^{dry} \times T} \tag{3.24}$$

$$N2O_{soil}^{dir} = rN2O \times \frac{N_{bio}^{dry} - N_{cr}^{dry} \times S_{cr}}{Y_{bio}^{dry}} \times GWP_{N2O}^{100yr} \tag{3.25}$$

$$rN2O = NV_N \times NV_{N2O} + V_N \times V_{N2O} \times \frac{(mole_N \times 2 + mole_o)}{mole_N} \tag{3.26}$$

$$Y_{bio}^{dry} = \frac{Y_{bio}^{wet}}{1 - mf_{H2O}^{wet}} \tag{3.27}$$

$$Y_{bio}^{dry,G} = Y_{bio}^{dry} \times (1 + ratio_{residue}) \tag{3.28}$$

$$C_{bio}^{abovegnd} = \frac{mf_c^{wet}}{1 - mf_{H2O}^{wet}} \tag{3.29}$$

$$C_{bio}^{root} = Y_{bio}^{dry} \times ratio_{R2S} \times C_{bio}^{abovegnd} \tag{3.30}$$

$$C_{biofcr}^{soil} = \left(AC_{bio}^{soil} - AC_{cr}^{soil}\right) \times T \tag{3.31}$$

$$C_{biofpa}^{soil} = \left(AC_{bio}^{soil} - AC_{pa}^{soil}\right) \times T \tag{3.32}$$

Indirect Land Use Change

$$S_{crfoth} = S_{cr} \times ratio_{ILUC/DLUC} \times F_{oth2cr} \tag{3.33}$$
$$S_{crfpa} = S_{cr} \times ratio_{ILUC/DLUC} \times (1 - F_{oth2cr}) \tag{3.34}$$
$$S_{pafoth} = S_{pa} \times ratio_{ILUC/DLUC} \tag{3.35}$$
$$\begin{aligned} EF_{bio}^{iluc} = {} & \Big(S_{crfoth} \times \left(CO_{2crfoth}^{abovegnd} + CO_{2crfoth}^{belowgnd} + CO_{2crfoth}^{soil}\right) + S_{crfpa} \\ & \times \left(CO_{2crfpa}^{abovegnd} + CO_{2crfpa}^{belowgnd} + CO_{2crfpa}^{soil}\right) + S_{pafoth} \\ & \times \left(CO_{2pafoth}^{abovegnd} + CO_{2pafoth}^{belowgnd} + CO_{2pafoth}^{soil}\right) + N2O_{soil}^{ind}\Big) \\ & \times \left(1 + loss_{bio}^{gnd}\right) \times (1 + loss_{bio}^{tor}) \times (1 - mf_{H2O}^{wet}) \end{aligned} \tag{3.36}$$

$$CO_{2crfoth}^{abovegnd} = \frac{44}{12} \times \frac{-\left[\left(fb \times Tb \times Y_{cr}^{dry,G} \times C_{cr}^{abovegnd}\right) - C_{oth}^{abovegnd}\right]}{Y_{bio}^{dry} \times T} \tag{3.37}$$

$$CO_{2crfpa}^{abovegnd} = \frac{44}{12} \times \frac{-\left[\left(fb \times Tb \times Y_{cr}^{dry,G} \times C_{cr}^{abovegnd}\right) - \left(fb \times Tb \times Y_{pa}^{dry,G} \times C_{pa}^{abovegnd}\right)\right]}{Y_{bio}^{dry} \times T} \tag{3.38}$$

$$CO_{2pafoth}^{abovegnd} = \frac{44}{12} \times \frac{-\left[\left(fb \times Tb \times Y_{pa}^{dry,G} \times C_{pa}^{abovegnd}\right) - C_{oth}^{abovegnd}\right]}{Y_{bio}^{dry} \times T} \tag{3.39}$$

$$CO_{2crfoth}^{belowgnd} = \frac{44}{12} \times \frac{-(C_{cr}^{root} - C_{oth}^{root})}{Y_{bio}^{dry} \times T} \tag{3.40}$$

$$CO_{2crfpa}^{belowgnd} = \frac{44}{12} \times \frac{-(C_{cr}^{root} - C_{pa}^{root})}{Y_{bio}^{dry} \times T} \tag{3.41}$$

$$CO_{2pafoth}^{belowgnd} = \frac{44}{12} \times \frac{-(C_{pa}^{root} - C_{oth}^{root})}{Y_{bio}^{dry} \times T} \tag{3.42}$$

$$CO_{2crfoth}^{soil} = \frac{44}{12} \times \frac{-C_{crfoth}^{soil}}{Y_{bio}^{dry} \times T} \tag{3.43}$$

$$CO_{2crfpa}^{soil} = \frac{44}{12} \times \frac{-C_{crfpa}^{soil}}{Y_{bio}^{dry} \times T} \tag{3.44}$$

$$CO_{2pafoth}^{soil} = \frac{44}{12} \times \frac{-C_{pafoth}^{soil}}{Y_{bio}^{dry} \times T} \tag{3.45}$$

$$N2O_{soil}^{ind} = rN2O \times \frac{N_{cr}^{dry} \times (S_{crfoth} + S_{crfpa})}{Y_{bio}^{dry}} \times GWP_{N2O}^{100yr} \tag{3.46}$$

GHG Emissions of Biomass Production

$$EF_{bio}^{production} = Uptake_{CO_2} + EF_{bio}^{cultivation} \quad (3.47)$$

CO₂ Uptake

$$Uptake_{CO2,ec,fr} = -\frac{44}{12} \times mf_{c}^{wet} \times \left(1 + loss_{bio}^{gnd}\right) \times \left(1 + loss_{bio}^{tor}\right) \quad (3.48)$$

$$Y^{wet} = Y_{re}^{wet} \times \frac{p \times (1 - HI) + HI}{p \times (1 - HI)} \quad (3.49)$$

$$EFactor_{allo} = \frac{HHV_{re} \times Y_{re}^{wet}}{HHV_{re} \times Y_{re}^{wet} + HHV_{pr} \times Y_{pr}^{wet}} \quad (3.50)$$

$$Uptake_{CO2,re} = -\frac{44}{12} \times \frac{Y_{re}^{wet} \times mf_{c,re}^{wet} + Y_{pr}^{wet} \times mf_{c,pr}^{wet}}{Y^{wet}} \times EFactor_{allo} \times \left(1 + loss_{bio}^{gnd}\right) \quad (3.51)$$

$$Y_{pr}^{wet} = Y^{wet} - Y_{re}^{wet} \quad (3.52)$$

Cultivation

$$EF_{bio}^{cultivation} = \left(EF_{dsluse}^{cultivation} + EF_{fertuse}^{cultivation} + EF_{herbuse}^{cultivation}\right) \times EFactor_{allo} \times \left(1 + loss_{bio}^{gnd}\right) \times \left(1 + loss_{bio}^{tor}\right) \quad (3.53)$$

$$U_{dc} = FU \times \left(\frac{DT}{DW \times DS} + \frac{PT}{PW \times PS}\right) \times \frac{T}{GC} \times \frac{F^{hatft2}}{F^{miletft}} \times F^{gatliter} \times F^{litertkg} \div T \quad (3.54)$$

$$EF_{dsluse}^{cultivation} = Diesel_{use} \times \frac{E_{diesel}}{Y^{wet}} \quad (3.55)$$

$$EF_{fertuse}^{cultivation} = \frac{N_{bio}^{wet}}{Y^{wet}} \times rN2O \times GWP_{N2O}^{100yr} \quad (3.56)$$

$$EF_{herbuse}^{cultivation} = \frac{U_h}{Y^{wet}} \times E_{herbicide} \quad (3.57)$$

GHG Emissions of Biomass Harvesting

$$EF_{bio}^{harvest} = U_{dh} \times E_{diesel} \times EFactor_{allo} \times \left(1 + loss_{bio}^{gnd}\right) \times \left(1 + loss_{bio}^{tor}\right) \quad (3.58)$$

$$U_{dh,hp} = \left(\frac{FC \times HPE \times F^{lbtliter}}{HWH \times HD} + \frac{FUT \times F^{gatliter}}{BW \times TO}\right) \times \frac{F^{hatft2} \times F^{litertkg}}{F^{miletft} \times Y^{wet}} \quad (3.59a)$$

$$U_{dh,hr} = \left(\frac{FC \times HPE \times F^{lbtliter}}{HWH \times HD}\right) \times \frac{F^{hatft2} \times F^{litertkg}}{F^{miletft} \times Y^{wet}} \quad (3.59b)$$

$$U_{dh,wp,wr} = \left(\frac{FC \times HPE \times F^{lbtliter}}{Area_H}\right) \times \frac{F^{litertkg}}{Y^{wet}} \quad (3.59c)$$

GHG Emissions of Biomass Processing

$$EF_{bio}^{process} = \begin{cases} EF_{bio}^{grind} \\ EF_{bio}^{torref} \end{cases} \quad (3.60)$$

$$EF_{bio}^{grind} = U_e \times E_e \times F^{MJtMWh} \quad (3.61)$$

$$EF_{bio}^{torref} = (E_{CO2} + E_{CH4} + E_{N2O}) \times (1 + loss_{bio}^{tor}) + U_e \times Ratio_{usel} \times E_e \times F^{MJtMWh} \quad (3.62)$$

GHG Emissions of Biomass Transport

$$EF_{bio}^{transport} = EF_{train}^{transport} \times D_{bio}^{train} + EF_{truck}^{transport} \times D_{bio}^{truck} + EF_{barge}^{transport} \times D_{bio}^{barge} \quad (3.63)$$

Table 3.5. Inputs of Land Use Change Emission Estimation.

Feedstock	**Symbol**	**Value**	**Unit**	**Source of Data**
Switchgrass	mf_{H2O}^{wet}	0.0921	fraction	Bush et al. (2001)
	mf_{c}^{wet}	0.4204	fraction	Bush et al. (2001)
	Y^{wet}	8819	kg/hectare/year	NETL (2010a), Bush et al. (2001)
	$ratio_{residue}$	0.22	fraction	Skone et al. (2011)
	N_{bio}^{dry}	112	kg N/hectare/year	Skone et al. (2011)
	$ratio_{R2S}$	1.69	fraction	Sainju et al. (2017)
	AC_{bio}^{soil}	788	kg C/hectare/year	Bai et al. (2020), Liebig et al. (2008)
	$loss_{bio}^{gnd}$	1.20E-05	fraction	NETL (2011b)
	$loss_{bio}^{tor}$	0	fraction	Not Applicable
Miscanthus	mf_{H2O}^{wet}	0.1454	fraction	EPRI (2010)
	mf_{c}^{wet}	0.4036	fraction	EPRI (2010)
	Y^{wet}	22296	kg/hectare/year	Jacobson (2013)
	$ratio_{residue}$	0.26	fraction	Kahle et al. (2001)
	N_{bio}^{dry}	83	kg N/hectare/year	Jacobson (2013), Song et al. (2016), Dumortier (2018), EPRI (2010)
	$ratio_{R2S}$	0.39	fraction	Mann et al. (2013)
	AC_{bio}^{soil}	770	kg C/hectare/year	Bazrgar et al. (2020)
	$loss_{bio}^{gnd}$	1.20E-05	fraction	NETL (2011b)
	$loss_{bio}^{tor}$	0	fraction	Not Applicable
Hybrid Poplar	mf_{H2O}^{wet}	0.0520	fraction	Zygarlicke et al. (2001)
	mf_{c}^{wet}	0.4503	fraction	Zygarlicke et al. (2001)
	Y^{wet}	12533	kg/hectare/year	NETL (2022), Zygarlicke et al. (2001)
	$ratio_{residue}$	0.50	fraction	Derrick (2023)
	N_{bio}^{dry}	67	kg N/hectare/year	NETL (2022), Zygarlicke et al. (2001)

	$ratio_{R2S}$	0.14	fraction	Fortier et al. (2015)
	AC_{bio}^{soil}	775	kg C/hectare/year	Rytter (2012), Bazrgar et al. (2020)
	$loss_{bio}^{gnd}$	1.20E-05	fraction	NETL (2011b)
	$loss_{bio}^{tor}$	0	fraction	Not Applicable
Willow (before torrefaction)	mf_{H2O}^{wet}	0.0890	fraction	Bridgeman et al. (2010)
	mf_{c}^{wet}	0.4417	fraction	Bridgeman et al. (2010)
	Y^{wet}	12075	kg/hectare/year	Caslin et al. (2015a)
	$ratio_{residue}$	0.50	fraction	Assumption based on Derrick (2023)
	N_{bio}^{dry}	123	kg N/hectare/year	Jacobson (2014), ESF (2017)
	$ratio_{R2S}$	0.22	fraction	Quinkenstein et al. (2012)
	AC_{bio}^{soil}	790	kg C/hectare/year	Rytter (2012), Bazrgar et al. (2020)
	$loss_{bio}^{tor}$	0.33	fraction	NETL (2012d)
Torrefied Wood[1,2,3]	$mf_{c,TW}^{wet}$	0.5793	fraction	Bridgeman et al. (2010)
	$ratio_{c}$	0.7625	fraction	Bridgeman et al. (2010)
Assumptions	fb	0.5	fraction	Skone et al. (2011)
	Tb	1	year	Skone et al. (2011)
	T	30	year	Skone et al. (2011)
	$C_{cr}^{abovegnd}$ / $C_{pa}^{abovegnd}$	0.4	kg C/kg	Skone et al. (2011)
	N_{cr}^{dry}	50	kg N/hectare/year	Skone et al. (2011)
	$Y_{cr}^{dry,G}$	1000	kg/hectare/year	Skone et al. (2011)
	$Y_{pa}^{dry,G}$	5000	kg/hectare/year	Skone et al. (2011)
	C_{cr}^{root}	2000	kg C/hectare	Skone et al. (2011)
	C_{pa}^{root}	4800	kg C/hectare	Skone et al. (2011)
	C_{oth}^{root}	10000	kg C/hectare	Skone et al. (2011)
	AC_{cr}^{soil}	553	kg C/hectare/year	Zomer et al. (2017)
	AC_{pa}^{soil}	665	kg C/hectare/year	Franzluebbers and Stuedemann (2009)
	C_{crfoth}^{soil}	-10853	kg C/hectare	Mayer et al. (2022), Zomer et al. (2017). Franzluebbers and Stuedemann (2009)
	C_{crfpa}^{soil}	-3350	kg C/hectare	
	C_{pafoth}^{soil}	-7503	kg C/hectare	
	$ratio_{ILUC/DLUC}$	0.3	fraction	Skone et al. (2011)
	F_{oth2cr}	0.5	fraction	Skone et al. (2011)
	$C_{oth}^{abovegnd}$	40000	kg C/hectare	Skone et al. (2011)
	S_{cr}	0.239	fraction	Skone et al. (2011)
	NV_{N}	0.9	fraction	Skone et al. (2011)
	NV_{N2O}	0.125	fraction	Skone et al. (2011)

	V_N	0.1	fraction	Skone et al. (2011)
	V_{N2O}	0.01	fraction	Skone et al. (2011)

Footnotes:
1. Torrefied wood refers to willow processed through torrefaction;
2. The properties of willow after torrefaction are embedded into the IECM;
3. In general, the properties of raw willow are used for GHG emission estimation. The $ratio_c$ should be considered when the properties of torrefied wood are used for GHG emission estimation.

Table 3.6. Inputs of CO_2 Uptake Estimation.

Feedstock	**Symbol**	**Value**	**Unit**	**Source of Data**
Switchgrass	mf_c^{wet}	0.4204	fraction	Bush et al. (2001)
	$loss_{bio}^{gnd}$	1.20E-05	fraction	NETL (2011b)
Miscanthus	mf_c^{wet}	0.4036	fraction	EPRI (2010)
	$loss_{bio}^{gnd}$	1.20E-05	fraction	NETL (2011b)
Hybrid Poplar	mf_c^{wet}	0.4503	fraction	Zygarlicke et al. (2001)
	$loss_{bio}^{gnd}$	1.20E-05	fraction	NETL (2011b)
Willow (before torrefaction)	mf_c^{wet}	0.4417	fraction	Bridgeman et al. (2010)
	$loss_{bio}^{tor}$	0.33	fraction	NETL (2012d)
Torrefied Wood[1,2,3]	$mf_{c,TW}^{wet}$	0.5793	fraction	Bridgeman et al. (2010)
	$ratio_c$	0.7625	fraction	Bridgeman et al. (2010)
Corn Stover	$mf_{c,re}^{wet}$	0.4124	fraction	ECN (2022)
	$mf_{c,pe}^{wet}$	0.3825	fraction	ECN (2022)
	Y_{re}^{wet}	405	kg/hectare/year	NETL (2010b)
	HHV_{re}	16230	kJ/kg	NETL (2010b)
	HHV_{pr}	16210	kJ/kg	NETL (2010b)
	HI	0.57	fraction	NETL (2010b)
	P	0.35	fraction	NETL (2010b)
	$loss_{bio}^{gnd}$	1.20E-05	fraction	NETL (2011b)
Wheat Straw	$mf_{c,re}^{wet}$	0.4300	fraction	EPRI (2012)
	$mf_{c,pe}^{wet}$	0.4265	fraction	EPRI (2012)
	Y_{re}^{wet}	253	kg/hectare/year	USDA (2024)
	HHV_{re}	16887	kJ/kg	EPRI (2012)
	HHV_{pr}	16901	kJ/kg	ECN (2022)
	HI	0.45	fraction	Dai et al. (2016)
	P	0.4	fraction	Scarlat et al. (2010)
	$loss_{bio}^{gnd}$	1.20E-05	fraction	NETL (2011b)
Forestry Residue	mf_c^{wet}	0.4791	fraction	ECN (2022)
	$loss_{bio}^{gnd}$	1.20E-05	fraction	NETL (2011b)

Footnotes:
1. Torrefied wood refers to willow processed through torrefaction;

2. The properties of willow after torrefaction are embedded into the IECM;
3. In general, the properties of raw willow are used for GHG emission estimation. The $ratio_c$ should be considered when the properties of torrefied wood are used for GHG emission estimation.

Table 3.7. Inputs of Biomass Cultivation Emission Estimation

Feedstock	Symbol	Value[1]	Unit	Source of Data
Switchgrass	GC	10	year	NETL (2010a)
	N_{bio}^{wet}	102	kg/hectare/year	Skone et al. (2011), Bush et al. (2001)
	U_h	2.62	kg/hectare/year	NETL (2010a)
	Y^{wet}	8819	kg/hectare/year	NETL (2010a), Bush et al. (2001)
	$loss_{bio}^{gnd}$	1.20E-05	fraction	NETL (2011b)
Miscanthus	GC	16	year	Winkler et al. (2020)
	N_{bio}^{wet}	71	kg/hectare/year	Jacobson (2013), Song et al. (2016), Dumortier (2018), EPRI (2010)
	U_h	2.16	kg/hectare/year	Caslin et al. (2015b)
	Y^{wet}	22296	kg/hectare/year	Jacobson (2013)
	$loss_{bio}^{gnd}$	1.20E-05	fraction	NETL (2011b)
Hybrid Poplar	U_{dc}	4.52	kg_{diesel}/hectare/year	NETL (2022)
	N_{bio}^{wet}	63	kg/hectare/year	NETL (2022)
	U_h	2.53	kg/hectare/year	NETL (2022)
	Y^{wet}	12533	kg/hectare/year	NETL (2022), Zygarlicke et al. (2001)
	$loss_{bio}^{gnd}$	1.20E-05	fraction	NETL (2011b)
Willow (before torrefaction)	GC	22	year	Jacobson (2014)
	N_{bio}^{wet}	112	kg/hectare/year	ESF (2017), Jacobson (2014)
	U_h	1.44	kg/hectare/year	Caslin et al. (2015a)
	Y^{wet}	12075	kg/hectare/year	Caslin et al. (2015a)
	$loss_{bio}^{tor}$	0.33	fraction	NETL (2012d)
Corn Stover[2]	GC	1	year	Assumption
	N_{bio}^{wet}	186	kg/hectare/year	NETL (2010b)
	U_h	0.93	kg/hectare/year	NETL (2010b)
	Y_{re}^{wet}	2473	kg/hectare/year	NETL (2010b)
	HI	0.57	fraction	NETL (2010b)
	P	0.35	fraction	NETL (2010b)
	$loss_{bio}^{gnd}$	1.20E-05	fraction	NETL (2011b)
Wheat Straw[2]	GC	1	year	Assumption
	N_{bio}^{wet}	87	kg/hectare/year	USDA (2022)
	U_h	0.92	kg/hectare/year	USDA (2024)
	Y_{re}^{wet}	1544	kg/hectare/year	USDA (2024)

	HI	0.45	fraction	Dai et al. (2016)
	P	0.4	fraction	Scarlat et al. (2010)
	$loss_{bio}^{gnd}$	1.20E-05	fraction	NETL (2011b)
Assumptions	FU	10.26	gallon/hour	NETL (2010a)
	DW	15.67	feet	NETL (2010a)
	DS	5.8	mile/hour	NETL (2010a)
	PW	40	feet	NETL (2010a)
	PS	5	mile/hour	NETL (2010a)
	DT	2	#	NETL (2010a)
	PT	1	#	NETL (2010a)
	V_N	0.1	fraction	NETL (2010a)
	NV_N	0.9	fraction	NETL (2010a)
	V_{N2O}	0.01	fraction	NETL (2010a)
	NV_{N2O}	0.0125	fraction	NETL (2010a)
	$E_{herbicide}$	16.46	kg CO_2eq/$kg_{herbicide}$	Camargo et al. (2013)
	T	30	year	Assumption

Footnotes:
1. The emission intensities associated with diesel consumption (E_{diesel}) are displayed in Tables S2.3;
2. The Y^{wet} can be calucated based on given Y_{re}^{wet}, HI, and P.

Table 3.8. Inputs of Biomass Harvesting Emission Estimation

Feedstock	Symbol	Value[1]	Unit	Source of Data
Switchgrass and Miscanthus	FC	0.34	lb_{diesel}/hp/hour	NETL (2010c)
	HPE	595	hp	NETL (2010c)
	HWH	15.02	feet	NETL (2010c)
	HD	6	mile/hour	NETL (2010c)
	FUT	10.26	gallon/hour	NETL (2010c)
	BW	9	feet	NETL (2010c)
	TO	5	mile/hour	NETL (2010c)
	Y^{wet}	8819 / 22296	kg/hectare/year	NETL (2010a), Bush et al. (2001), Jacobson (2013)
	$loss_{bio}^{gnd}$	1.20E-05	fraction	NETL (2011b)
Hybrid Poplar, Willow (before torrefaction), and Pine Spruce Chips	FC	0.35	lb_{diesel}/hp/hour	NETL (2010d)
	HPE	440	hp	NETL (2010d)
	$Area_H$	2.14	hectare/hour	Waratch (2024), Ecolog (2023), Xuvol (2024), Deere (2024), Tigercat (2024a), Tigercat (2024b), WoodsmanPro (2024), Komatsu (2024), Maskiner (2024)
	Y^{wet}	12533 / 12075 / 61537	kg/hectare/year	NETL (2022), Zygarlicke et al. (2001), Caslin et al. (2015a), Ghaffariyan and Dupuis (2021).
	$loss_{bio}^{gnd}$	1.20E-05	fraction	NETL (2011b)
	$loss_{bio}^{tor}$	0.33	fraction	NETL (2012d)
	FC	0.34	lb_{diesel}/hp/hour	NETL (2010e)

Corn Stover and Wheat Straw[2]	HPE	360	hp	NETL (2010e)
	HWH	7.92	feet	NETL (2010e)
	HD	5.5	mile/hour	NETL (2010e)
	Y_{re}^{wet}	2473 / 1544	kg/hectare/year	NETL (2010b), USDA (2024)
	$loss_{bio}^{gnd}$	1.20E-05	fraction	NETL (2011b)

Footnotes:
1. The emission intensities associated with diesel consumption (E_{diesel}) are displayed in Tables S2.3;
2. The Y^{wet} can be calculated based on given Y_{re}^{wet}, HI, and P.

Table 3.9. Inputs of Biomass Processing Emission Estimation

Feedstock	Symbol	Value[1]	Unit	Source of Data
All Biomass, except for Torrefied Wood	U_e	0.36	MJ/kg	NETL (2011b)
Torrefied Wood	E_{CO2}	5.25E-02	kg CO_2eq/kg_{bio-in}	NETL (2012d)
	E_{CH4}	4.2E-07	kg CH_4/kg_{bio-in}	NETL (2012d)
	E_{N2O}	4.1E-07	kg N_2O/kg_{bio-in}	NETL (2012d)
	$Ratio_{usel}$	0.05	fraction	NETL (2012d)
	$loss_{bio}^{tor}$	0.33	fraction	NETL (2012d)

Footnote:
1. The emission intensities associated with electricity consumption (E_e) are displayed in Tables S2.2.

Table 3.10. Biomass Supply Chain Emissions.

Biomass Category	**Energy Crop**				**Agricultural Residue**		**Forestry Residue**
Stage \ **Name**	**Switchgrass**	**Miscanthus**	**Hybrid Poplar**	**Torrefied Wood**	**Corn Stover**	**Wheat Straw**	**Pine Spruce Chips**
Direct Land Use Change (kg CO_2eq/kg_{bio})	-6.3E-02	-3.1E-02	-2.2E-02	-1.2E-02	0.0E+00	0.0E+00	0.0E+00
Indirect Land Use Change (kg CO_2eq/kg_{bio})	2.0E-01	7.8E-02	1.4E-01	1.9E-01	0.0E+00	0.0E+00	0.0E+00
CO_2 Uptake (kg CO_2eq/kg_{bio})	-1.5E+00	-1.5E+00	-1.7E+00	-2.2E+00	-3.0E-01	-5.1E-01	-1.8E+00
Cultivation (kg CO_2eq/kg_{bio})	5.5E-02	1.5E-02	2.6E-02	5.6E-02	1.5E-02	3.1E-02	0.0E+00
Harvesting (kg CO_2eq/kg_{bio})	1.6E-02	6.2E-03	1.0E-02	1.4E-02	1.7E-03	6.9E-03	2.1E-03
Processing (kg CO_2eq/kg_{bio})	5.9E-02	5.9E-02	5.9E-02	7.3E-02	5.9E-02	5.9E-02	5.9E-02
Transport (kg CO_2eq/kg_{bio}/km)							
By Train	2.0E-05						
By Truck	1.2E-04						
By Barge	2.7E-05						

The GHG emissions of the biomass supply depend on factors such as land use type, biomass property, yield, and processing requirements. For instance, the carbon content of biomass plays a key role in estimating CO_2 uptake during biomass growth. To clarify the relationship between GHG emissions and key variables, such as biomass properties and yield, certain equations are simplified and expressed as functions of these variables.

The simplification process consists of four steps. First, the main GHG emission sources that contribute to biomass supply emissions are identified. These sources are associated with biomass land use change, CO_2 uptake, cultivation, and harvesting, as outlined in Equations (3.17) to (3.59). Second, numerical values from Tables 3.5 to 3.9, excluding the values for key variables, are input into the above equations. Third, these values are combined to form simplified expressions, as presented in Equations (3.64) to (3.91). Finally, the simplified equations are embedded into the IECM.

Simplified GHG Emission Estimation Equations for Switchgrass

$$\mathrm{EF_{bio}^{dluc}} = -0.2813 \times \mathrm{mf_c^{wet}} + \frac{0.2145 - 0.3597 \times \mathrm{S_{cr}} + 0.1149 \times \mathrm{S_{pr}}}{\mathrm{Z^{wet}}} \tag{3.64}$$

$$\mathrm{EF_{bio}^{iluc}} = \frac{2.819 \times \mathrm{S_{pr}} + 1.8841 \times \mathrm{S_{cr}}}{\mathrm{Z^{wet}}} \times \mathrm{ratio_{ILUC/DLUC}} \tag{3.65}$$

$$\mathrm{Uptake_{CO2}} = -\frac{44}{12} \times \mathrm{mf_c^{wet}} \tag{3.66}$$

$$\mathrm{EF_{bio}^{cultivation}} = \frac{0.2171}{\mathrm{Z^{wet}}} \tag{3.67}$$

$$\mathrm{EF_{bio}^{harvest}} = \frac{0.06129}{\mathrm{Z^{wet}}} \tag{3.68}$$

Simplified GHG Emission Estimation Equations for Miscanthus

$$\mathrm{EF_{bio}^{dluc}} = -0.1246 \times \mathrm{mf_c^{wet}} + \frac{0.1594 - 0.3301 \times \mathrm{S_{cr}} + 0.1445 \times \mathrm{S_{pr}}}{\mathrm{Z^{wet}}} \tag{3.69}$$

$$\mathrm{EF_{bio}^{iluc}} = \frac{2.819 \times \mathrm{S_{pr}} + 1.8841 \times \mathrm{S_{cr}}}{\mathrm{Z^{wet}}} \times \mathrm{ratio_{ILUC/DLUC}} \tag{3.70}$$

$$\mathrm{Uptake_{CO2}} = -\frac{44}{12} \times \mathrm{mf_c^{wet}} \tag{3.71}$$

$$\mathrm{EF_{bio}^{cultivation}} = \frac{0.1542}{\mathrm{Z^{wet}}} \tag{3.72}$$

$$\mathrm{EF_{bio}^{harvest}} = \frac{0.06129}{\mathrm{Z^{wet}}} \tag{3.73}$$

Simplified GHG Emission Estimation Equations for Hybrid Poplar

$$\mathrm{EF_{bio}^{dluc}} = -0.1088 \times \mathrm{mf_c^{wet}} + \frac{0.1272 - 0.3383 \times \mathrm{S_{cr}} + 0.1363 \times \mathrm{S_{pr}}}{\mathrm{Z^{wet}}} \tag{3.74}$$

$$\mathrm{EF_{bio}^{iluc}} = \frac{2.819 \times \mathrm{S_{pr}} + 1.8841 \times \mathrm{S_{cr}}}{\mathrm{Z^{wet}}} \times \mathrm{ratio_{ILUC/DLUC}} \tag{3.75}$$

$$\mathrm{Uptake_{CO2}} = -\frac{44}{12} \times \mathrm{mf_c^{wet}} \tag{3.76}$$

$$\mathrm{EF}_{\mathrm{bio}}^{\mathrm{cultivation}} = \frac{0.1470}{Z^{\mathrm{wet}}} \tag{3.77}$$

$$\mathrm{EF}_{\mathrm{bio}}^{\mathrm{harvest}} = \frac{0.05634}{Z^{\mathrm{wet}}} \tag{3.78}$$

Simplified GHG Emission Estimation Equations for Torrefied Wood

$$\mathrm{EF}_{\mathrm{bio}}^{\mathrm{dluc}}\left(= -0.1185 \times \mathrm{ratio}_{\mathrm{c}} \times \mathrm{mf}_{\mathrm{c,TW}}^{\mathrm{wet}} + \frac{0.2354 - 0.3628 \times S_{\mathrm{cr}} + 0.1118 \times S_{\mathrm{pr}}}{Z^{\mathrm{wet}}}\right) \times (1 + \mathrm{loss}_{\mathrm{bio}}^{\mathrm{tor}}) \tag{3.79}$$

$$\mathrm{EF}_{\mathrm{bio}}^{\mathrm{iluc}} = \frac{2.819 \times S_{\mathrm{pr}} + 1.8841 \times S_{\mathrm{cr}}}{Z^{\mathrm{wet}}} \times \mathrm{ratio}_{\mathrm{ILUC/DLUC}} \times (1 + \mathrm{loss}_{\mathrm{bio}}^{\mathrm{tor}}) \tag{3.80}$$

$$\mathrm{Uptake}_{\mathrm{CO2}} = -\frac{44}{12} \times \mathrm{ratio}_{\mathrm{c}} \times \mathrm{mf}_{\mathrm{c,TW}}^{\mathrm{wet}} \times (1 + \mathrm{loss}_{\mathrm{bio}}^{\mathrm{tor}}) \tag{3.81}$$

$$\mathrm{EF}_{\mathrm{bio}}^{\mathrm{cultivation}} = \frac{0.2264}{Z^{\mathrm{wet}}} \times (1 + \mathrm{loss}_{\mathrm{bio}}^{\mathrm{tor}}) \tag{3.82}$$

$$\mathrm{EF}_{\mathrm{bio}}^{\mathrm{harvest}} = \frac{0.05634}{Z^{\mathrm{wet}}} \times (1 + \mathrm{loss}_{\mathrm{bio}}^{\mathrm{tor}}) \tag{3.83}$$

Simplified GHG Emission Estimation Equations for Corn Stover

$$\mathrm{Uptake}_{\mathrm{CO2}} = -\frac{44}{12} \times \frac{\mathrm{mf}_{\mathrm{c,re}}^{\mathrm{wet}} + \frac{\mathrm{HI}}{p \times (1 - \mathrm{HI})} \times \mathrm{mf}_{\mathrm{c,pr}}^{\mathrm{wet}}}{1 + \frac{\mathrm{HI}}{p \times (1 - \mathrm{HI})}} \times \frac{1}{1 + \frac{\mathrm{HHV}_{\mathrm{pr}}}{\mathrm{HHV}_{\mathrm{re}}} \times \frac{\mathrm{HI}}{p \times (1 - \mathrm{HI})}} \tag{3.84}$$

$$\mathrm{EF}_{\mathrm{bio}}^{\mathrm{cultivation}} = \frac{0.3930}{Z_{\mathrm{re}}^{\mathrm{wet}} \times \left(1 + \frac{\mathrm{HI}}{p \times (1 - \mathrm{HI})}\right)} \times \frac{1}{1 + \frac{\mathrm{HHV}_{\mathrm{pr}}}{\mathrm{HHV}_{\mathrm{re}}} \times \frac{\mathrm{HI}}{p \times (1 - \mathrm{HI})}} \tag{3.85}$$

$$\mathrm{EF}_{\mathrm{bio}}^{\mathrm{harvest}} = \frac{0.04478}{Z_{\mathrm{re}}^{\mathrm{wet}} \times \left(1 + \frac{\mathrm{HI}}{p \times (1 - \mathrm{HI})}\right)} \times \frac{1}{1 + \frac{\mathrm{HHV}_{\mathrm{pr}}}{\mathrm{HHV}_{\mathrm{re}}} \times \frac{\mathrm{HI}}{p \times (1 - \mathrm{HI})}} \tag{3.86}$$

Simplified GHG Emission Estimation Equations for Wheat Straw

$$\mathrm{Uptake}_{\mathrm{CO2}} = -\frac{44}{12} \times \frac{\mathrm{mf}_{\mathrm{c,re}}^{\mathrm{wet}} + \frac{\mathrm{HI}}{p \times (1 - \mathrm{HI})} \times \mathrm{mf}_{\mathrm{c,pr}}^{\mathrm{wet}}}{1 + \frac{\mathrm{HI}}{p \times (1 - \mathrm{HI})}} \times \frac{1}{1 + \frac{\mathrm{HHV}_{\mathrm{pr}}}{\mathrm{HHV}_{\mathrm{re}}} \times \frac{\mathrm{HI}}{p \times (1 - \mathrm{HI})}} \tag{3.87}$$

$$\mathrm{EF}_{\mathrm{bio}}^{\mathrm{cultivation}} = \frac{0.2051}{Z_{\mathrm{re}}^{\mathrm{wet}} \times \left(1 + \frac{\mathrm{HI}}{p \times (1 - \mathrm{HI})}\right)} \times \frac{1}{1 + \frac{\mathrm{HHV}_{\mathrm{pr}}}{\mathrm{HHV}_{\mathrm{re}}} \times \frac{\mathrm{HI}}{p \times (1 - \mathrm{HI})}} \tag{3.88}$$

$$\mathrm{EF}_{\mathrm{bio}}^{\mathrm{harvest}} = \frac{0.04478}{Z_{\mathrm{re}}^{\mathrm{wet}} \times \left(1 + \frac{\mathrm{HI}}{p \times (1 - \mathrm{HI})}\right)} \times \frac{1}{1 + \frac{\mathrm{HHV}_{\mathrm{pr}}}{\mathrm{HHV}_{\mathrm{re}}} \times \frac{\mathrm{HI}}{p \times (1 - \mathrm{HI})}} \tag{3.89}$$

Simplified GHG Emission Estimation Equations for Pine Spruce Chips

$$\text{Uptake}_{\text{CO2}} = -\frac{44}{12} \times \text{mf}_{\text{c}}^{\text{wet}} \tag{3.90}$$

$$\text{EF}_{\text{bio}}^{\text{harvest}} = \frac{0.05634}{\text{Z}^{\text{wet}}} \tag{3.91}$$

(b) Combustion-Based Power Generation

A combustion-based power plant burns fuel and consumes natural resources to generate electricity for the grid. Meanwhile, the power plant emits GHG into the atmosphere. The GHG emissions from the power plant operation refer specifically to the plant-level CO_2 stack emissions. The GHG emissions for the electricity generation plant are estimated using the IECM model.

(c) CO_2 Transport and Storage

Captured CO_2 in a power plant is compressed to a supercritical state, transported via pipeline to a CO_2 storage location, and then injected underground for geological storage. The CO_2 transport and storage (T&S) include pipeline transport and geological storage, as shown in Equation (3.92). The GHG emissions for CO_2 T&S are estimated using the method of NETL unit process files (NETL, 2012e–2012j) as well as consumption rates and consumption emission intensities of energy and material (NETL, 2011a, 2014, 2023; Skone et al., 2013, 2018b). The calculation details for pipeline transport and geological storage are listed in Equations (3.93) to (3.104). Tables 3.11 and 3.12 summarize the input and the GHG emissions results for CO_2 T&S, respectively.

Pipeline Transport. GHG emissions of CO_2 transport stem from pipeline construction and operation. Key emission sources include pipeline fugitive, pipeline pigging, and CO_2 pump leakage (Skone et al., 2018b).

Geological Storage. Storage emissions are estimated based on the hypothetical storage location in the Permian Basin (Skone et al., 2013), assuming a 30-year project lifetime. GHG emissions of CO_2 storage stem from saline aquifer well assembly (including well construction and closure), storage site preparation, monitoring, operation, brine management, seal leakage, and formation leakage.

GHG Emissions of CO_2 Transport and Storage

$$\text{EF}_{\text{T\&S}} = \text{EF}_{\text{CO2}}^{\text{Transport}} + \text{EF}_{\text{CO2}}^{\text{Storage}} \tag{3.92}$$

GHG Emissions of Pipeline Transport

$$\text{EF}_{\text{CO2}}^{\text{Transport}} = \text{E}_{\text{fugitive}}^{\text{Transport}} + \text{E}_{\text{pig}}^{\text{Transport}} + \text{E}_{\text{pumpleak}}^{\text{Transport}} + \text{E}_{\text{construction}}^{\text{Transport}} \tag{3.93}$$

$$\text{E}_{\text{fugitive}}^{\text{Transport}} = \frac{\text{Leak}_{\text{CO2}} \times \text{Fugiative}_{\text{CH4}} \times \text{Density}_{\text{CO2}}}{\text{F}^{\text{yrtdy}} \times \text{F}^{\text{kmtmi}}} \times \frac{\text{L}_{\text{pipe}}}{\text{Deliver}_{\text{CO2}}} \times \text{F}^{\text{kgtMT}} \tag{3.94}$$

$$\text{E}_{\text{pig}}^{\text{Transport}} = 8.82 \times 10^{-11} \times \left(\frac{\text{L}_{\text{pipe}}}{\text{F}^{\text{kmtmi}}} \times 1000\right)^{1.339} \tag{3.95}$$

$$\text{Power}_{\text{pump}} = 0.0001867 \times \text{Deliver}_{\text{CO2}} \tag{3.96}$$

$$E_{pumpleak}^{Transport} = \frac{E_{pump} \times Power_{pump}}{Deliver_{CO2}} \times F^{kgtMT} \quad (3.97)$$

$$D_{pipe} = 0.0222 \times L_{pipe} + 14.8 \quad (3.98)$$

$$Density_{pipeline} = 1175.6 \times D_{pipe}{}^{2} + 87.13 \times D_{pipe} + 29915 \quad (3.99)$$

$$E_{construction}^{Transport} = \frac{Density_{pipeline} \times L_{pipe}}{Deliver_{CO2} \times F^{yrtdy} \times Period_{pipe}} \times \left(1 + Tortuosity_{pipe}\right) \times \left(1 + weight_{pipe}\right) \times E_{steel} \times F^{kgtMT} \quad (3.100)$$

GHG Emissions of Geological Storage

$$EF_{CO2}^{storage} = E_{formleak}^{storage} + E_{wellconstruction}^{storage} + E_{suvery}^{storage} + C_{e}^{storage} \times E_{e} + C_{diesel}^{storage} \times Area_{survey} \times E_{diesel} \quad (3.101)$$

$$E_{wellconstruction}^{storage} = \frac{\sum Num_{well} \times \left(Steel_{well} \times E_{steel} + C_{diesel}^{consSt} \times E_{diesel} + E_{GHG}^{constru}\right) \times F^{kgtMT}}{Deliver_{CO2} \times F^{yrtdy} \times Period_{pipe}} \quad (3.102)$$

$$C_{diesel}^{consSt} = U_{d} \times \frac{Drill_{depth} \times Drill_{power}}{Drill_{speed}} \quad (3.103)$$

$$E_{suvery}^{storage} = Area_{survey} \times E_{survery} \quad (3.104)$$

Table 3.11. Input Parameter for CO_2 Transport and Storage Emission Estimation.

Stage[1]	**Symbol**	**Value**	**Unit**	**Source of Data**
Transport	$Leak_{CO2}$	0.6	unitless	NETL (2012e)
	$Fugiative_{CH4}$	2000	m^3/km-yr	NETL (2012e)
	$Density_{CO2}$	1.98	kg/m^3	NETL (2012e)
	L_{pipe}	100	mile	NETL (2012e)
	$Deliver_{CO2}$	11,000	tonnes/day	NETL (2012e)
	$Tortuosity_{pipe}$	0.05	unitless	NETL (2013f)
	$weight_{pipe}$	0.05	unitless	NETL (2013f)
	$Period_{pipe}$	30	year	NETL (2013f)
	E_{pump}	180	kg/MW-day	NETL (2012f)
Storage	$E_{formleak}^{storage}$	0.005	kg CO_2eq/kg CO_2	Skone et al. (2013)
	Num_{well}	2–15, depending on well type[2]	# of well	NETL (2012f)
	$Steel_{well}$	1.0E+5	kg_{steel}/well	NETL (2012g)
	U_{d}	221	kg_{diesel}/MWh	NETL (2012h)
	$Drill_{depth}$	12.2–2620, depending on well type	m/well	Skone et al. (2013)
	$Drill_{power}$	0.45	MW	NETL (2012h)
	$Drill_{speed}$	17.8	m/h	NETL (2012h)

	$E_{GHG}^{constru}$	217–46600, depending on well type	kg CO_2eq/well	NETL (2012j)
	$Area_{survey}$	6.2E-10	km^2/kg CO_2	NETL (2012j)
	$E_{survery}$	3.8E+03	kg CO_2eq/km^2	NETL (2012i)
	$C_{e}^{storage}$	1.3E-05	MWh/kg CO_2	Skone et al. (2013)
	$C_{diesel}^{storage}$	1.2E+3	kg_{diesel}/km^2	NETL (2012j)

Footnotes:

1. The emission intensities associated with electricity (E_e), diesel (E_{diesel}), and steel (E_{steel}) consumption are displayed in Tables S2.2 to S2.4, respectively;
2. The well types include stratigraphic test well, injection well, in-reservoir monitoring well, above seal monitoring well, groundwater monitoring well, vadose zone monitoring well, water production well, and water disposal well.

Table 3.12. CO_2 Transport and Storage Emissions.

Stage	**Emissions**
Pipeline Transport (kg CO_2eq/kg $CO_{2\text{-captured}}$/km)[1]	1.1E-05
Geological Storage (kg CO_2eq/kg $CO_{2\text{-captured}}$)	1.3E-02

Footnote:

1. Pipeline transport GHG emissions are embedded into IECM as kg CO_2eq/kg $CO_{2\text{-captured}}$, with a default transport distance of 100 km.

Section 4: Case Study

This section consists of 2 parts: (1) “Input Parameter and Assumption” outlines the technical parameters and key assumptions in the power plant configurations of the coal-fired and coal-biomass co-firing power plants, and (2) “Major Result” presents the technical performance and life cycle emissions of the studied cases, including the coal-fired plants without and with CCS, biomass co-firing plants without and with CCS.

4.1 Input Parameter and Assumption

The coal resources examined in the case study include Illinois No. 6 (IL6) and Powder River Basin (PRB) coal. The IL6 is a bituminous coal, while PRB is a subbituminous coal. The biomass resources include seven biomass samples from energy crops, agricultural residues, and forestry residues. Tables 1.1 and 1.3 list the properties of coal and biomass, respectively. The bituminous coal has a much higher heating value and larger carbon content. Additionally, torrefied wood and pine spruce chips exhibit relatively high heating values and large carbon content, followed by hybrid poplar, switchgrass, wheat straw, corn stover, and miscanthus. Fuel property comparison indicates that IL6 exhibits more favorable combustion characteristics compared to PRB, and energy crops and forestry residues generally have better combustion characteristics than agricultural residues. Better fuel property leads to better power plant performance.

The GHG emissions for plant operation mainly depend on plant size, configuration, and process design. Hypothetical pulverized coal (PC) power plants in Illinois and Wyoming serve as reference plants. The reference PC plants are assumed to be supercritical, with a capacity factor of 75%, a lifetime of 30 years, and a gross capacity of 650 MWg. The plants employ wet cooling towers and are equipped with air pollution control systems, including Electrostatic Precipitator (ESP), Selective Catalytic Reduction (SCR), and Flue Gas Desulfurization (FGD).

In addition, we explore the impact of biomass co-firing and CCS implementation by configuring coal-biomass co-firing power plants. The gross capacity is kept the same for all plants. Coal is co-fired with biomass on a 20% energy basis. An amine-based, post-combustion CCS of 90% or 95% CO_2 capture rate is included in the plant. Table 4.1 summarizes the vital technical parameters and configuration assumptions for the power plants.

Table 4.1. Major Parameters and Assumptions for Pulverized Coal or Co-Firing Plants without and with CCS.

Parameter	**Value**	**Parameter**	**Value**
Base Plant:		*Cooling System:*	Wet Cooling Tower
Power Plant Location	Illinois and Wyoming	*Traditional Air Pollution Control Systems:*	
Plant Type	Supercritical	NO_x Control	Selective Catalytic Reduction
Gross Capacity (MW_g)	650	Particulate Control	Electrostatic Precipitator
Capacity Factor (%)	75	SO_2 Control	Flue Gas Desulfurization

Production Technology	Pulverized Coal Power Plant	*Carbon Capture and Storage (Whenever Applicable):*	
Co-Firing Level (%, energy basis)	20	CO_2 Capture Technology	Amine
Fuel Transport:		Amine Concentration (wt.%)	30
Coal Transport Method	Train	CO_2 Capture Efficiency (%)	90 and 95
Coal Transport Round-Trip Distance (km)[1]	644	CO_2 Transport Method	Pipeline
Biomass Transport Method	Truck	CO_2 Transport (km)	161
Biomass Transport Round-Trip Distance (km)[2]	644 for IL, 1000 for WY	CO_2 Storage Method	Geological Sequestration

Footnotes:
1. The coal transport distance is estimated based on Skone et al. (2018a);
2. The biomass transport distance is estimated based on the biomass availability reported by Milbrandt (2005).

4.2 Major Result

(a) PC Power Plants without and with CCS

Based on the IECM simulation results, the IL6 PC plant has 6% higher net plant efficiency, 1% higher net power output, 32% lower fuel consumption rate (Figure 4.1), and 9% less stack GHG emissions than the PRB PC plant. Stack GHG emissions from both PC plants are more than 800 kg CO_2/MWh (Figure 4.2). The differences between the two power plants are mainly due to IL6 being bituminous coal with better combustion characteristics. This leads to less parasitic load on the power plant during electricity generation. In addition, the PRB PC plant consumes more fuel to maintain the same gross capacity. As a result, the PRB PC plant’s stack emissions are slightly higher than those of the IL6 PC plant.

Compared to PC plants without CCS, the deployment of CCS with a 90% CO_2 capture rate results in a 29% reduction in plant net efficiency, a 14% reduction in net generation, and a 42% increase in fuel consumption rate (Figure 4.1). Increasing the CO_2 capture rate from 0% to 95% results in a 30% reduction in net efficiency, a 15% reduction in net generation, and requires a 45% increase in fuel consumption rate. However, the implementation of CCS does reduce plants’ stack GHG emissions by 90–95%. The addition of a CO_2 capture system significantly affects plant operation performance and fuel consumption rate due to the large parasitic load associated with CCS operation, but the CCS can largely reduce stack emissions (Figure 4.2).

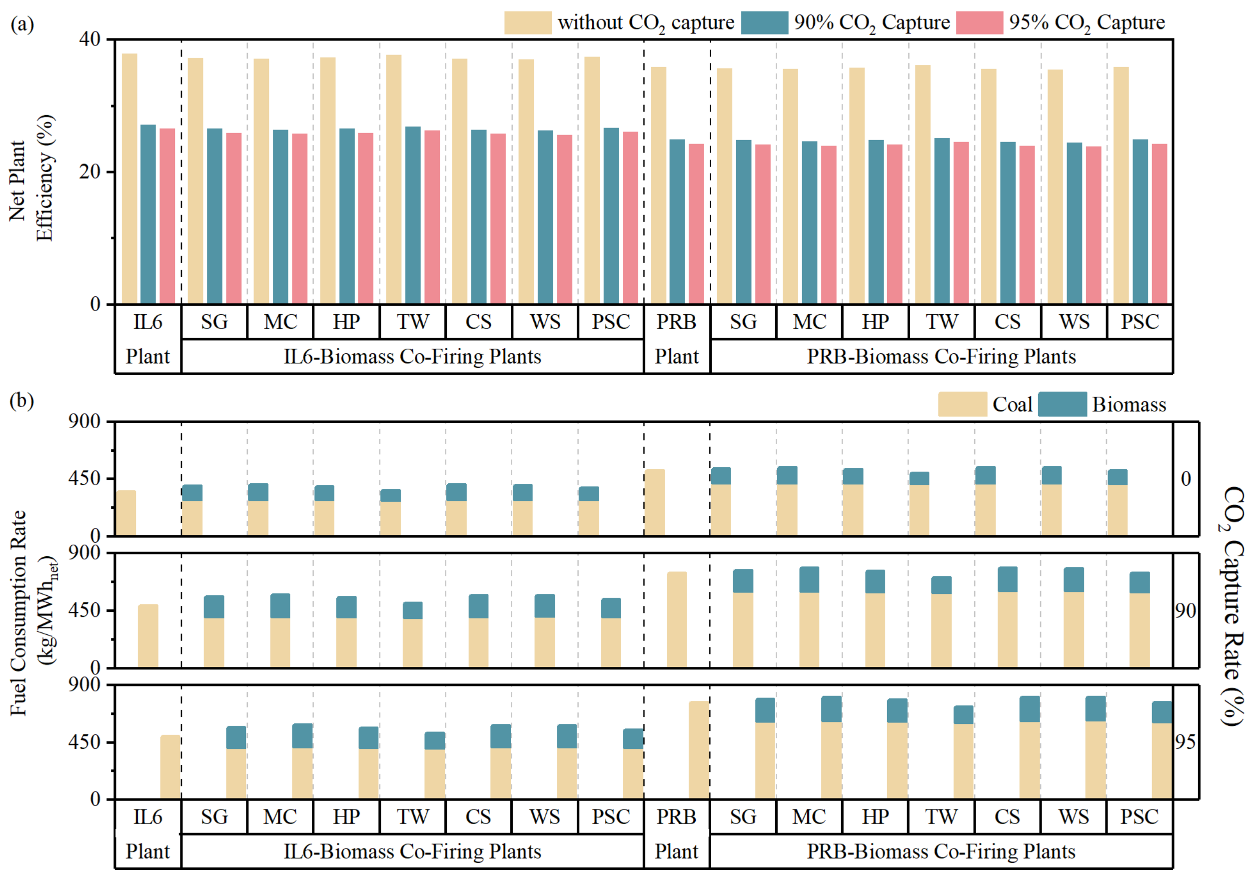

Figure 4.1. Performance of 20% Co-Firing Power Plants without and with CCS: (a) Net Plant Efficiency, and (b) Fuel Consumption Rate.

(b) Coal-Biomass Co-Firing Power Plants without and with CCS

Compared to PC plants without CCS, biomass co-firing plants show a 1% decrease in net plant efficiency, a 0.2% reduction in net power output, and an 8% increase in fuel consumption rate, while reducing life cycle emissions by 12% (Figures 4.1 and 4.2). Biomass co-firing slightly affects the technical performance of power plants but reduces their life cycle emissions. The results show that stack emissions from plant operation are the dominant source of life cycle emissions at co-firing plants without CCS (Figure 4.2), accounting for over 90% of life cycle emissions. The implementation of biomass reduces life cycle emissions due to its negative supply emissions.

The study also evaluates the implementation of 90–95% CCS to the co-firing power plants. Compared to co-firing plants without CCS, deploying CCS with a 90% and 95% CO_2 capture rate reduces net plant efficiency by 30% and 31%, respectively. Additionally, the co-firing plants' net power output decreases by 14% and 15%, while fuel requirements increase by 42% and 46%, respectively. From a life cycle perspective, deploying a CCS system to co-firing power plants with 20% biomass can reduce GHG emissions by an average of 97% and 104% under 90% and 95% CO_2 capture rates (Figure 4.2), respectively. The net-zero life cycle emissions can be reached if coal is fired with switchgrass, miscanthus, hybrid poplar, torrefied wood, or pine spruce chip at power plants with a 95% CO_2 capture rate.

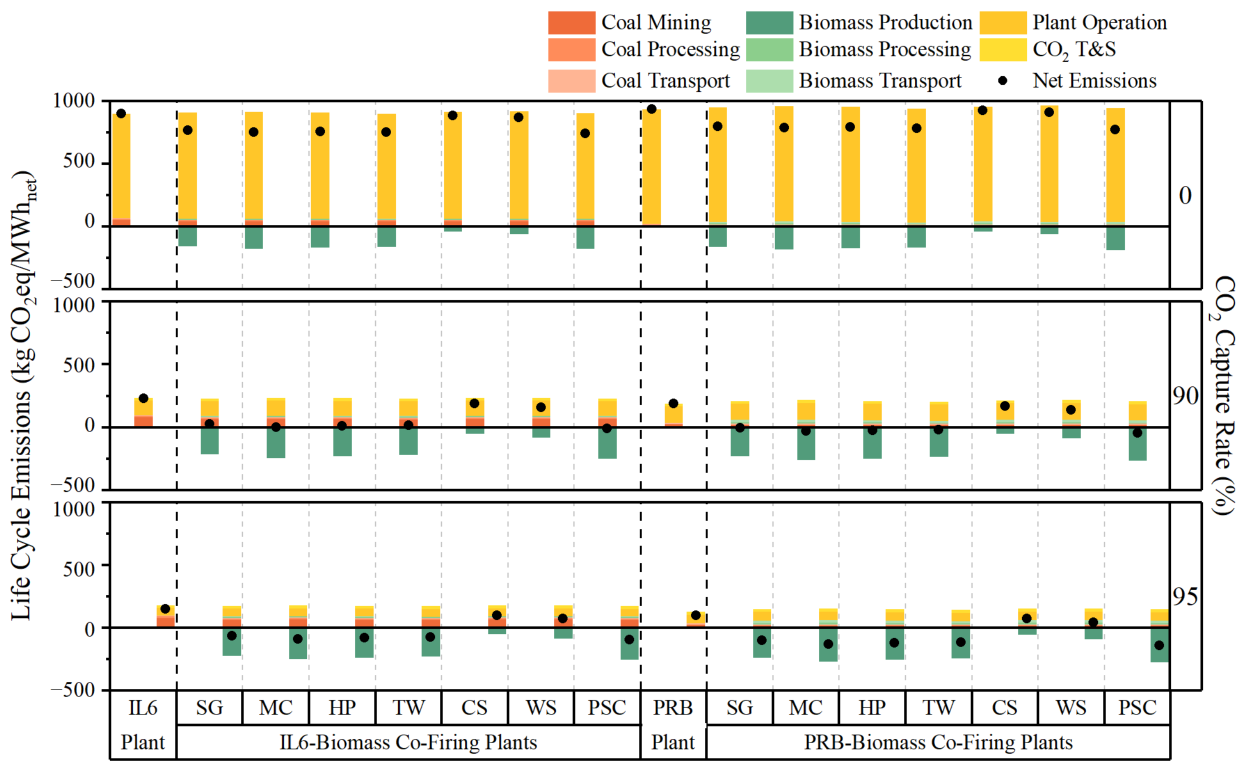

Figure 4.2. Life Cycle Emissions of 20% Co-Firing Power Plants without and with CCS.

The evaluation results imply that implementing both biomass and CCS offers an opportunity for co-firing power plants to achieve net-zero life cycle emissions. A distribution diagram is created to show the contribution of each stage to the total life cycle emissions, with all emission results treated as absolute values. Based on the life cycle emissions distribution (Figure 4.3), coal supply and plant operation contribute the most to overall life cycle emissions, while biomass supply provides significant reductions in emissions.

Comparison between Figures 4.3a and 4.3b shows that IL6 coal supply emissions contribute 16–31% of overall life cycle emissions at coal-biomass co-firing power plants, which is 2–3 times more than PRB coal. Plant operation emissions distribution is similar between the two types of coal power plants. The life cycle emissions of the co-firing plants vary across biomass types, coal types, and CO_2 capture rates.

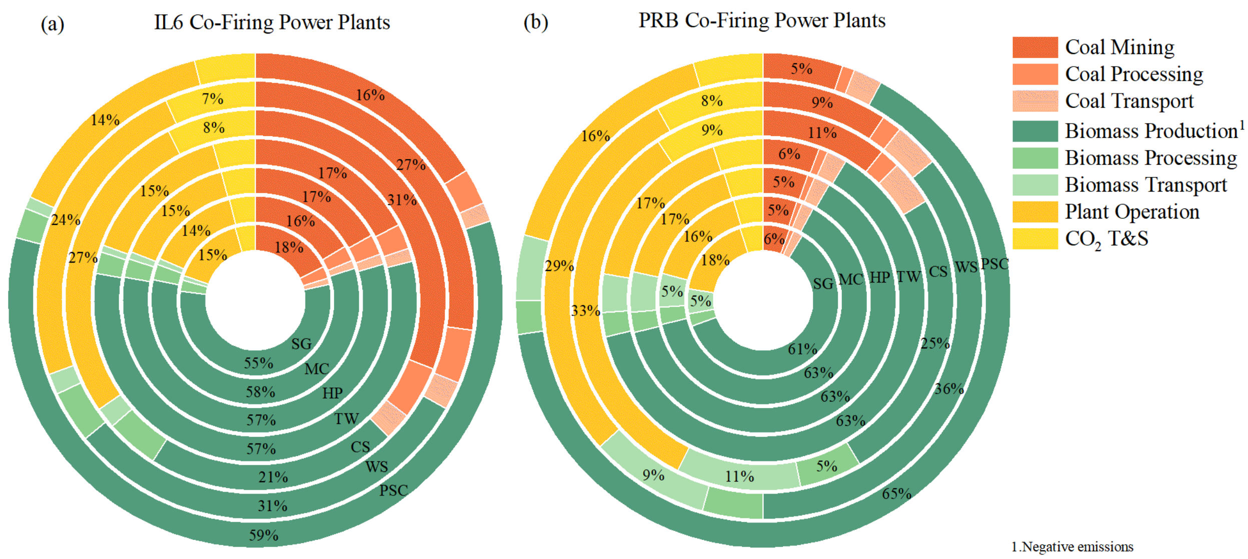

Figure 4.3. Life Cycle Emissions Distribution of Coal-Biomass Co-Firing Power Plants with 95% CO_2 Capture Rate: (a) Illinois No. 6 Coal Co-Fired with Biomass, and (b) Powder River Basin Coal Co-Fired with Biomass.

(c) Breakeven Biomass Co-Firing Level for Net-Zero Emissions

We also examine the relationship between the required breakeven co-firing level and biomass types, coal types as well as CO_2 capture rates.

Biomass Types. The breakeven co-firing levels of each biomass type show only a slight variation, with a 1–2% difference. The breakeven co-firing levels are determined based on biomass properties and supply emissions. Figure 4.4 shows the breakeven co-firing levels for the five biomass samples from energy crops and forestry residues, since agricultural residue cannot achieve net-zero emissions at a breakeven co-firing level below 30%. These results suggest that energy crops and forestry residues have a larger carbon sequestration potential than that of agricultural residues. Among five biomass samples, pine spruce chips achieve net-zero emissions at the lowest co-firing level (10–14%, energy basis), while miscanthus has the highest required co-firing level (11–15%, energy basis). On the other hand, torrefied wood required the lowest mass basis breakeven co-firing level, while switchgrass required the highest mass basis co-firing level. This indicates that biomass with a higher heating value and greater carbon content requires lower levels of breakeven co-firing to achieve net-zero emissions.

Coal Types. The breakeven co-firing level is also affected by the coal properties and supply emissions. IL6 coal, for instance, has a relatively higher heating value and larger carbon content but significantly higher supply emissions than PRB coal, primarily due to the methane emissions from underground mining. Biomass co-firing at IL6 power plants, thus, requires a relatively higher breakeven co-firing level. This highlights the importance of mitigating upstream methane emissions in coal mining processes.

CO_2 Capture Rates. Increasing the capture rate from 90% to 95% effectively lowers the breakeven co-firing level by an absolute 5%. Deploying CCS with a 95% CO_2 capture rate can lead to breakeven net-zero life cycle emissions at biomass co-firing levels ranging from 10% to 16% on the energy basis (Figure 4.4).

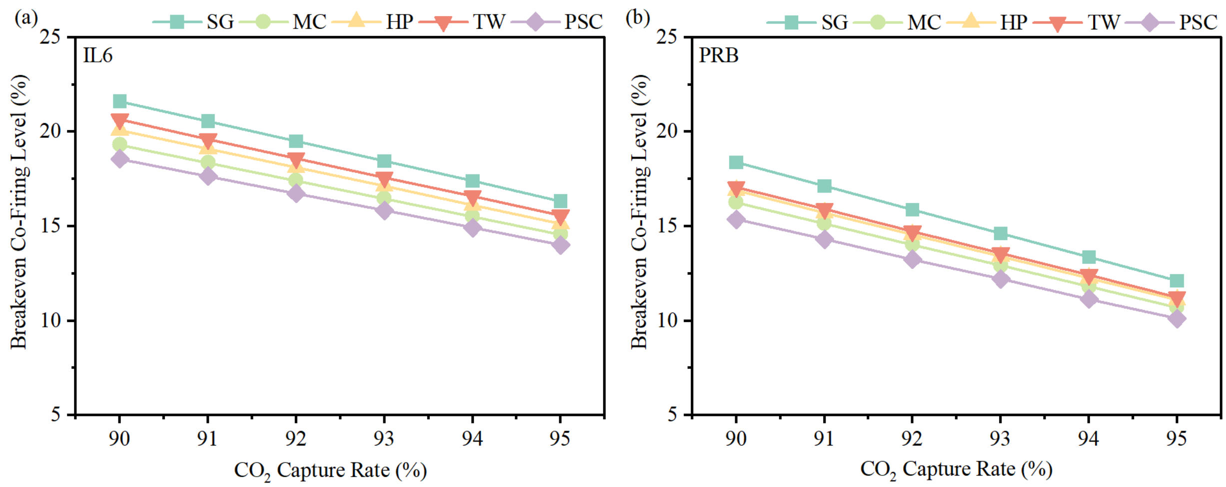

Figure 2.4. Life Cycle Emissions of 20% Co-Firing Power Plants with CCS for 95% CO_2 Capture: (a) Illinois No. 6 Coal Co-Fired with Biomass, and (b) Powder River Basin Coal Co-Fired with Biomass.

Summary

This document organizes the updates to the IECM into four sections.

The "Fuel Database" section describes a function and database for users to configure a power plant that combusts multiple fuels. To configure a co-firing plant, users first need to specify the fuel blend percentages. They can then enter the property of more than one fuel. The fuel can either be selected from the existing fuel database or custom as needed.

The "Boiler Efficiency Algorithm" section outlines the overall boiler efficiency calculation formula. The IECM takes into account the property of each fuel to compute the boiler efficiency of a power plant.

The "Life Cycle GHG Emission Model" section explains GHG emission estimation methods for both fuel supply and CO_2 T&S. For fuels, the model includes options for two coal samples, one waste coal sample, and seven biomass samples. For CO_2 T&S, the model includes pipeline transport and geological storage. If a custom fuel is entered, its higher heating value is used to determine the closest matching fuel proxy for calculating fuel supply GHG emissions. If the CO_2 pipeline transport distance is not specified, the default pipeline length is used to calculate the CO_2 T&S GHG emissions.

The "Case Study" section presents the key inputs, assumptions, and results of the technical performance and environmental impacts of co-firing power plants.

References

- American Society of Mechanical Engineers (ASME). (1964). ASME PTC 4.1-1976. Steam Generating Units.
- Bai, J., Luo, L., Li, A., Lai, X., Zhang, X., Yu, Y., Wang, H., Wu, N. & Zhang, L. (2022). Effects of Biofuel Crop Switchgrass (Panicum Virgatum) Cultivation on Soil Carbon Sequestration and Greenhouse Gas Emissions: A Review. *Life*, 12(12), 2105
- Bazrgar, A. B., Ng, A., Coleman, B., Ashiq, M. W., Gordon, A., and Thevathasan, N. (2020). Long-Term Monitoring of Soil Carbon Sequestration in Woody and Herbaceous Biofuel Production Systems on Marginal Lands in Southern Ontario, Canada. *Sustainability*, 12(9), 3901.
- Black, J. B., Haslbeck, J. L., Lewis, E., Woods, M. C., and Matuszewski, M. (2012). Greenhouse Gas Reductions in the Power Industry using Domestic Coal and Biomass - volume 1: IGCC (No. DOE/NETL-2012/1546). National Energy Technology Laboratory
- Bridgeman, T. G., Jones, J. M., Williams, A., and Waldron, D. J. (2010). An Investigation of the Grindability of Two Torrefied Energy Crops. *Fuel*, 89(12), 3911-3918.
- Buchheit, K. Lewis, E. Mahbubani, K. and Carlson. D. (2021). Technoeconomic and Life Cycle Analysis of Bio-Energy with Carbon Capture and Storage (BECCS) Baseline. National Energy Technology Laboratory.
- Bureau of Labor Statistics. (2023). Consumer Price Index. Available at https://www.bls.gov/cpi/questions-and-answers.htm Accessed at 03.28.2023.
- Bush, P. V., Boylan, D. M., Bransby, D. I., Smith, H. A., and Taylor, C. R. (2001). Evaluation of Switchgrass as a Co-Firing Fuel in the Southeast. DOE Cooperative Agreement No. DE-FC36-98GO10349. EPRI WO# 4603-05.

- Camargo, G.G.T., Ryan, M.R., Richard, T.L. (2013). Energy Use and Greenhouse Gas Emissions from Crop Production using the Farm Energy Analysis Tool. *BioScience*, 63, 263-273.
- Caslin B., Finnan J., Johnston C., McCracken A., Walsh L. (2015a) Short Rotation Coppice Willow Best Practice Guidelines. ISBN number 1-84170-610-8.
- Caslin B., Finnan J., Johnston C. (2015b). Miscanthus Best Practice Guidelines. ISBN number 1-84170-611-5.
- Cutshaw, A., Carlson, D. R., Henriksen, M., Krynock, M., Jamieson, M., and James III, R. E. (2023). Cradle-to-Gate Life Cycle Analysis Baseline for United States Coal Mining and Delivery (No. DOE/NETL-2024/4846). National Energy Technology Laboratory.
- Dai, J., Bean, B., Brown, B., Bruening, W., Edwards, J., Flowers, M., Karow, R., Lee, C., Morgan, G., Ottman, M. and Ransom, J. (2016). Harvest Index and Straw Yield of Five Classes of Wheat. *Biomass and Bioenergy*, 85, 223-227.
- Deere (2024). 1270G Wheeled Harvester. Available at https://www.deere.com/en/wheeled-harvesters/1270g/
- Derrick, C. (2023). Personal Communication for Coal and Biomass Emissions Estimation for 'Technoeconomic and Life Cycle Analysis of Bio-Energy with Carbon Capture and Storage (BECCS) Baseline' Report.
- Dumortier, J. (Chapter Author) Li, Ruopu, and Andrea Monti (Eds). (2018) Land Allocation for Biomass Crops: Challenges and Opportunities with Changing Land Use.
- Ecolog (2023) Harvester Head 461 LF, 561 LF, 661 LF & 761 LF. Available at https://ecologforestry.com/wp-content/uploads/2023/10/eco-log-aggregat-broschyr_web_eng.pdf
- Electric Power Research Institute (EPRI) (2010). Vista Program Capabilities for Analysis of Biomass Co-Firing. EPRI, Palo Alto, CA: 2010. 1020682.
- Electric Power Research Institute (EPRI) (2012). Program on Technology Innovation: Gasification Testing of Various Biomasses in Untreated and Pretreated (Leached) Forms. EPRI, Palo Alto, CA: 2012. 1024893.
- Electric Power Research Institute (EPRI). (2008). Engineering and Economic Evaluation of 1300°F Series Ultra-Supercritical Pulverized Coal Power Plants: Phase 1. Palo Alto, CA: 2008. 1015699.
- Electric Power Research Institute (EPRI). (2018) Engineering-Economic Evaluations of Advanced Fossil Fuel Power Plants with Carbon Capture and Storage. EPRI, Palo Alto, CA: 2018. 3002013869.
- Energy Information Administration (EIA). (2023). Coal Data Explorer, Available at https://www.eia.gov/coal/data/browser/#/topic/44?agg=1,0&geo=nvg1qag9vvlpnu&rank=02&linechart=COAL.SHIP_MINE_PRICE.US-WC.A&columnchart=COAL.SHIP_MINE_PRICE.US-WC.A&map=COAL.SHIP_MINE_PRICE.US-WC.A&freq=A&start=2008&end=2021&ctype=linechart&ltype=sourcekey&rtype=s&maptype=0&rse=0&pin= Accessed in 03.22.2023.
- Energy Research Centre of the Netherlands (ECN). (2022). Phyllis2, database for (treated) biomass, algae, feedstocks for biogas production and biochar. Available at https://phyllis.nl/

- Environmental Science and Forestry (ESF). (2014) Opportunities for Rural Development. Available at https://www.esf.edu/willow/
- Facanha, C. and Horvath, A. (2007). Evaluation of Life Cycle Air Emissions of Freight Transportation. *Environmental Science & Technology*, 41(20), 7138-7144
- Federal LCA Commons. (2020). Coal Transport-Barge. Available at https://www.lcacommons.gov/lca-collaboration/Federal_LCA_Commons/US_electricity_baseline/dataset/PROCESS/4921deff-38c1-3912-b780-4b95870312f4
- Fortier, J., Truax, B., Gagnon, D., and Lambert, F. (2015). Plastic Allometry in Coarse Root Biomass of Mature Hybrid Poplar Plantations. *BioEnergy Research*, 8, 1691-1704.
- Franzluebbers, A. J. and Stuedemann, J. A. (2009). Soil-Profile Organic Carbon and Total Nitrogen During 12 years of Pasture Management in the Southern Piedmont USA. *Agriculture, Ecosystems & Environment*, 129(1-3), 28-36.
- Ghaffariyan, M. R. and Dupuis, E. (2021). Analysing the Impact of Harvesting Methods on the Quantity of Harvesting Residues An Australian Case Study. *Forests*, 12(9), 1212.
- Grammelis, P., Skodras, G., and Kakaras, E. (2006). Effects of Biomass Co-Firing with Coal on Ash Properties. Part I: Characterisation and PSD. *Fuel*, 85(16), 2310-2315.
- Hanak, D. P. (2022). Environmental Life Cycle Assessment of Waste-Coal Pellets Production. *Clean Energy*, 6(1), 1-14
- Integrated Environmental Control Model. (2019a). IECM Technical Documentation: Integrated Gasification Combined Cycle Power Plants.
- Integrated Environmental Control Model. (2019b). IECM Technical Documentation: Pulverized Coal-Fired Power Plants and Air Pollution Controls. https://www.uwyo.edu/iecm/_bfiles/documentation/201903_iecmtd_cp-apc-rev-a.pdf.
- Integrated Environmental Control Model. (2021). Integrated Environmental Control Model (IECM) Version 11.5 (Carnegie Mellon University). https://www.cmu.edu/epp/iecm/index.html.
- Intergovernmental Panel on Climate Change (IPCC). (2014), Climate Change 2014: Synthesis Report. Contribution of Working Groups I, II and III to the Fifth Assessment Report of the Intergovernmental Panel on Climate Change, IPCC, Geneva, 2014.
- International Renewable Energy Agency (IRENA). (2015). Renewable power generation costs in 2014. Available at https://www.irena.org/-/media/Files/IRENA/Agency/Publication/2015/IRENA_RE_Power_Costs_2014_report.pdf?rev=4dfc65cc95394824805d5449babc2c93 Access at 03.26.2023
- Irving, W. and Tailakov, O. (2000). CH_4 Emissions: Coal Mining and Handling. In Background Papers IPCC Expert Meetings on Good Practice Guidance and Uncertainty Management in National Greenhouse Gas Inventories (pp. 129-144). Available at https://www.ipcc-nggip.iges.or.jp/public/gp/bgp/2_7_Coal_Mining_Handling.pdf
- Jacobson, M. (2014). Shrub Willow Budget for Biomass Production.
- Jacobson, M., Marrison, D., Helsel, Z., Rak, D., Forgeng, B. and Heil, N. (2013) Renewables and Alternative Energy Fact Sheet.
- Kahle, P., Beuch, S., Boelcke, B., Leinweber, P., and Schulten, H. R. (2001). Cropping of Miscanthus in Central Europe: Biomass Production and Influence on Nutrients and Soil Organic Matter. *European Journal of Agronomy*, 15(3), 171-184.

- Kolker, A., Scott, C.T., Croke, M.R., Lefticariu, L., Mastalerz, M., Drobniak, A., and Scott, A.M. (2021) Geochemical Data for Illinois Basin Coal Samples, 2015–2018 (ver. 1.1, March 2021): U.S. Geological Survey Data Release, Available at https://doi.org/10.5066/P9GUURCK.
- Komatsu (2024). Harvesting Head C124. Available at https://www.komatsu.com/en/products/forestry/harvester-heads/c124/#specifications
- Kopczyński, M., Lasek, J. A., Iluk, A., and Zuwała, J. (2017). The Co-Combustion of Hard Coal with Raw and Torrefied Biomasses (Willow (Salix Viminalis), Olive Oil Residue and Waste Wood from Furniture Manufacturing). *Energy*, 140, 1316-1325
- Kumar, A., Cameron, J. B., and Flynn, P. C. (2005). Pipeline Transport and Simultaneous Saccharification of Corn Stover. *Bioresource Technology*, 96(7), 819-829.
- Liebig, M. A., Schmer, M. R., Vogel, K. P., and Mitchell, R. B. (2008). Soil Carbon Storage by Switchgrass Grown for Bioenergy. *Bioenergy Research*, 1, 215-222.
- Mahmudi, H., and Flynn, P. C. (2006). Rail vs Truck Transport of Biomass. In Twenty-Seventh Symposium on Biotechnology for Fuels and Chemicals (pp. 88-103). Humana Press.
- Mann, J. J., Barney, J. N., Kyser, G. B., and Di Tomaso, J. M. (2013). Miscanthus× Giganteus and Arundo Donax Shoot and Rhizome Tolerance of Extreme Moisture Stress. *Gcb Bioenergy*, 5(6), 693-700.
- Maskiner (2024) Harvester Head SP 661 LF - Technical data. Available at https://spmaskiner.com/en/harvester-heads/harvester-heads-lf/harvester-head-sp-661-lf/sp-661-lf-technical-data/
- Mayer, S., Wiesmeier, M., Sakamoto, E., Hübner, R., Cardinael, R., Kühnel, A., and Kögel-Knabner, I. (2022). Soil Organic Carbon Sequestration in Temperate Agroforestry Systems A Meta-Analysis. *Agriculture, Ecosystems & Environment*, 323, 107689
- Miedema, J. H., Benders, R. M., Moll, H. C., and Pierie, F. (2017). Renew, Reduce or Become More Efficient? The Climate Contribution of Biomass Co-Combustion in a Coal-Fired Power Plant. *Applied Energy*, 187, 873-885.
- Milbrandt, A. (2005). Geographic Perspective on the Current Biomass Resource Availability in the United States (No. NREL/TP-560-39181). National Renewable Energy Lab. (NREL), Golden, CO (United States).
- Mun, T. Y., Tumsa, T. Z., Lee, U., and Yang, W. (2016). Performance Evaluation of Co-Firing Various Kinds of Biomass with Low Rank Coals in a 500 MW_e Coal-Fired Power Plant. *Energy*, 115, 954-962.
- National Energy Technology Laboratory (NETL). (2007). Cost and Performance Baseline for Fossil Energy Plants. Report No. DOE/NETL-2007/1281.
- National Energy Technology Laboratory (NETL). (2009). NETL Life Cycle Inventory Data – Unit Process: Underground Mine, Illinois No. 6 Bituminous Coal, Operation.
- National Energy Technology Laboratory (NETL). (2010). NETL Life Cycle Inventory Data – Process Data Sheet File: Train Transport - Unspecified, Operations. U.S. Department of Energy, National Energy Technology Laboratory. Last Updated: February 2010 (version 01). www.netl.doe.gov/energy-analyses (http://www.netl.doe.gov/energy-analyses)

- National Energy Technology Laboratory (NETL). (2010a). NETL Life Cycle Inventory Data – Unit Process: Switchgrass Cultivation, Operation. U.S. Department of Energy, National Energy Technology Laboratory. Last Updated: December 2014 (version 03). www.netl.doe.gov/energy-analyses (http://www.netl.doe.gov/energy-analyses)
- National Energy Technology Laboratory (NETL). (2010b). NETL Life Cycle Inventory Data – Unit Process: Corn Stover Cultivation, Operation. U.S. Department of Energy, National Energy Technology Laboratory. Last Updated: December 2014 (version 03). www.netl.doe.gov/energy-analyses (http://www.netl.doe.gov/energy-analyses)
- National Energy Technology Laboratory (NETL). (2010c). NETL Life Cycle Inventory Data – Unit Process: Switchgrass Harvesting & Storage, operation. U.S. Department of Energy, National Energy Technology
- National Energy Technology Laboratory (NETL). (2010d). NETL Life Cycle Inventory Data – Unit Process: SRWC Harvesting & Storage, Operation. U.S. Department of Energy, National Energy Technology Laboratory. Last Updated: December 2014 (version 03).
- National Energy Technology Laboratory (NETL). (2010e). NETL Life Cycle Inventory Data – Unit Process: Corn Stover Harvesting & Storage, Operation. U.S. Department of Energy, National Energy Technology Laboratory. Last Updated: June 2012 (version 02). www.netl.doe.gov/energy-analyses (http://www.netl.doe.gov/energy-analyses)
- National Energy Technology Laboratory (NETL). (2011). NETL Life Cycle Inventory Data – Unit Process: Truck transport of spent uranium fuel. U.S. Department of Energy, National Energy Technology Laboratory. Last Updated: August 2011 (version 01). www.netl.doe.gov/energy-analyses (http://www.netl.doe.gov/energy-analyses)
- National Energy Technology Laboratory (NETL). (2011a). NETL Life Cycle Inventory Data – Unit Process: Diesel, Production, Transport, and Refining. U.S. Department of Energy, National Energy Technology Laboratory. Last Updated: May 2012 (version 02). www.netl.doe.gov/energy-analyses (http://www.netl.doe.gov/energy-analyses).
- National Energy Technology Laboratory (NETL). (2011b). NETL Life Cycle Inventory Data – Biomass Grinding for Coal-Biomass Cofiring, Operations. U.S. Department of Energy, National Energy Technology Laboratory. Last Updated: July 2011 (version 01). www.netl.doe.gov/energy-analyses (http://www.netl.doe.gov/energy-analyses)
- National Energy Technology Laboratory (NETL). (2012a). NETL Life Cycle Inventory Data – Unit Process: Land Use, Direct and Indirect. U.S. Department of Energy, National Energy Technology Laboratory. Last Updated: May 2012 (version 01). www.netl.doe.gov/energy-analyses (http://www.netl.doe.gov/energy-analyses)
- National Energy Technology Laboratory (NETL). (2012b). NETL Life Cycle Inventory Data – Unit Process: Southern Pine Cultivation, Operation. U.S. Department of Energy, National Energy Technology Laboratory. Last Updated: December 2014 (version 02). www.netl.doe.gov/energy-analyses (http://www.netl.doe.gov/energy-analyses)
- National Energy Technology Laboratory (NETL). (2012c). NETL Life Cycle Inventory Data – Unit Process: Southern Pine Harvesting & Storage, Operation. U.S. Department of Energy, National Energy Technology Laboratory. Last Updated: December 2014 (version 02). www.netl.doe.gov/energy-analyses (http://www.netl.doe.gov/energy-analyses)
- National Energy Technology Laboratory (NETL). (2012d). NETL Life Cycle Inventory Data – SRWC Biomass Torrefaction for Coal-Biomass Cofiring, Operation. U.S.

Department of Energy, National Energy Technology Laboratory. Last Updated: July 2012 (version 01). www.netl.doe.gov/energy-analyses (http://www.netl.doe.gov/energy-analyses)

- National Energy Technology Laboratory (NETL). (2012e). NETL Life Cycle Inventory Data – Unit Process: CO_2 Pipeline Operation. U.S. Department of Energy, National Energy Technology Laboratory. Last Updated: April 23, 2014 (version 02). www.netl.doe.gov/energy-analyses (http://www.netl.doe.gov/energy-analyses)
- National Energy Technology Laboratory (NETL). (2012f). NETL Life Cycle Inventory Data – Unit Process: CO_2 Pipeline Construction. U.S. Department of Energy, National Energy Technology Laboratory. Last Updated: October 2012 (version 01). www.netl.doe.gov/energy-analyses (http://www.netl.doe.gov/energy-analyses)
- National Energy Technology Laboratory (NETL). (2012g). NETL Life Cycle Inventory Data – Unit Process: Assembly, Saline Aquifer Well Construction, Installation and Closure. U.S. Department of Energy, National Energy Technology Laboratory. Last Updated: August 2012 (version 01). www.netl.doe.gov/energy-analyses (http://www.netl.doe.gov/energy-analyses)
- National Energy Technology Laboratory (NETL). (2012h). NETL Life Cycle Inventory Data – Carbon Dioxide Well Construction and Installation. U.S. Department of Energy, National Energy Technology Laboratory. Last Updated: November 2012 (version 01). www.netl.doe.gov/energy-analyses (http://www.netl.doe.gov/energy-analyses)
- National Energy Technology Laboratory (NETL). (2012i) Life Cycle Inventory Data – Unit Process: Vibroseis Truck Seismic Survey, Operation. U.S. Department of Energy, National Energy Technology Laboratory. Last Updated: October 2012 (version 01). www.netl.doe.gov/energy-analyses (http://www.netl.doe.gov/energy-analyses)
- National Energy Technology Laboratory (NETL). (2012j). NETL Life Cycle Inventory Data – Unit Process: Saline Aquifer CO_2 Injection Site Operations. U.S. Department of Energy, National Energy Technology Laboratory. Last Updated: September 2012 (version 01). www.netl.doe.gov/energy-analyses (http://www.netl.doe.gov/energy-analyses)
- National Energy Technology Laboratory (NETL). (2013a). NETL Life Cycle Inventory Data – Unit Process: Ventilation Energy for Underground Mine. U.S. Department of Energy, National Energy Technology Laboratory.
- National Energy Technology Laboratory (NETL). (2013b). NETL Life Cycle Inventory Data – Unit Process: Coal Handling Energy, Underground. U.S. Department of Energy, National Energy Technology Laboratory
- National Energy Technology Laboratory (NETL). (2013c). NETL Life Cycle Inventory Data – Unit Process: Coal Cleaning - Version 02. U.S. Department of Energy, National Energy Technology Laboratory.
- National Energy Technology Laboratory (NETL). (2013d). NETL Life Cycle Inventory Data – Unit Process: Surface Coal Mining – Overburden Removal, Extraction, and Reclamation. U.S. Department of Energy, National Energy Technology Laboratory. Last Updated: May 2015 (version 02). www.netl.doe.gov/LCA (http://www.netl.doe.gov/LCA)
- National Energy Technology Laboratory (NETL). (2013e). NETL Life Cycle Inventory Data – Unit Process: Coal Handling Energy, Surface. U.S. Department of Energy,

National Energy Technology Laboratory. Last Updated: July 2013 (version 01). www.netl.doe.gov/LCA (http://www.netl.doe.gov/LCA)

- National Energy Technology Laboratory (NETL). (2013f). NETL Life Cycle Inventory Data – Unit Process: CO_2 Pipeline Pigging. U.S. Department of Energy, National Energy Technology Laboratory. Last Updated: March 2013 (version 01). www.netl.doe.gov/LCA (http://www.netl.doe.gov/LCA)
- National Energy Technology Laboratory (NETL). (2014). NETL Life Cycle Inventory Data – Unit Process: Combustion of Diesel. U.S. Department of Energy, National Energy Technology Laboratory. Last Updated: January 2015 (version 02). www.netl.doe.gov/LCA (http://www.netl.doe.gov/LCA)
- National Energy Technology Laboratory (NETL). (2016). NETL Life Cycle Inventory Data – Unit Process: Steel products - Version 01. U.S. Department of Energy, National Energy Technology Laboratory. Retrieved [DATE] from www.netl.doe.gov/LCA
- National Energy Technology Laboratory (NETL). (2019). Quality Guidelines for Energy System Studies: Specification for Selected Feedstocks (No. NETL-PUB-22460). National Energy Technology Laboratory (NETL). (NETL), Pittsburgh, PA, Morgantown, WV, and Albany, OR (United States).
- National Energy Technology Laboratory (NETL). (2022). NETL Life Cycle Inventory Data – Unit Process: Hybrid Poplar Cultivation. U.S. Department of Energy, National Energy Technology Laboratory. Last Updated: April 2023 (version 01). www.netl.doe.gov/LCA
- National Energy Technology Laboratory (NETL). (2023) NETL CO_2U openLCA LCI Database Version 2.1 (https://www.lcacommons.gov/lca-collaboration/Federal_LCA_Commons/US_electricity_baseline/dataset/PROCESS/bac6bf3f-43f4-376d-9f16-bfe9740afa66)
- O'Connell, A., Pavlenko, N., Bieker, G., and Searle, S. (2023). A Comparison of the Life Cycle Greenhouse Gas Emissions of European Heavy-Duty Vehicles and Fuels. International Council on Clean Transportation: Washington, DC, USA, 1-36.
- Plevin, R. J., Jones, A. D., Torn, M. S., and Gibbs, H. K. (2010). Greenhouse Gas Emissions from Biofuels' Indirect Land Use Change Are Uncertain but May Be Much Greater than Previously Estimated. *Environmental Science & Technology*. 2010, 44, 21, 8015–8021.
- Pronobis, M., and Wojnar, W. (2013). The Impact of Biomass Co-Combustion on the Erosion of Boiler Convection Surfaces. *Energy Conversion and Management*, 74, 462-470.
- Quinkenstein, A., Pape, D., Freese, D., Schneider, B. U., and Hüttl, R. F. (2012). Biomass, Carbon and Nitrogen Distribution in Living Woody Plant Parts of Robinia pseudoacacia L. Growing on Reclamation Sites in the Mining Region of Lower Lusatia (Northeast Germany). *International Journal of Forestry Research*, 2012(1), 891798.
- Riley, J. T. (2014). Routine Coal and Coke Analysis: Collection, Interpretation, and Use of Analytical Data. Pennsylvania: ASTM International.
- Rytter, R. M. (2012). The Potential of Willow and Poplar Plantations as Carbon Sinks in Sweden. *Biomass and Bioenergy*, 36, 86-95.
- Sainju, U. M., Allen, B. L., Lenssen, A. W., and Ghimire, R. P. (2017). Root Biomass, Root/Shoot Ratio, and Soil Water Content under Perennial Grasses with Different Nitrogen Fates. *Field Crops Research*, 210, 183-191.

- Scarlat, N., Martinov, M., and Dallemand, J. F. (2010). Assessment of the Availability of Agricultural Crop Residues in the European Union: Potential and Limitations for Bioenergy Use. *Waste Management*, 30(10), 1889-1897.
- Singer, J. G. Eds. (1981). Combustion: Fossil Power Systems. Combustion Engineering Inc., Windsor, CT.
- Skone, T. J., and William H. (2011) Life Cycle Greenhouse Gas Analysis of Advanced Jet Propulsion Fuels: FT Based SPK-1 Case Study (Report). (No. AFRL-RZ-WP-TR-2011-2138). National Energy Technology Laboratory (NETL). (NETL), Pittsburgh, PA, Morgantown, WV, and Albany, OR (United States), 2011.
- Skone, T. J., Cooney, G., Marriott, J., Mutchek, M., and Krynock, M. (2016) Life cycle analysis of coal exports from the powder river basin. (No. DOE/NETL-2016/1806). National Energy Technology Laboratory. Pittsburgh, PA, Morgantown, WV, and Albany, OR (United States), 2016.
- Skone, T. J., James III, R. E., Cooney, G., Jamieson, M., Littlefield, J., and Marriott, J. (2013). Gate-to-Grave Life Cycle Analysis Model of Saline Aquifer Sequestration of Carbon Dioxide (No. DOE/NETL-2013/1600). National Energy Technology Laboratory. Pittsburgh, PA, Morgantown, WV, and Albany, OR (United States).
- Skone, T. J., Littlefield, J., Eckard, R., Cooney, G., Wallace, R., and Marriott, J. (2012). Role of alternative energy sources: pulverized coal and biomass co-firing technology assessment (No. NETL/DOE-2012/1537). National Energy Technology Laboratory. Pittsburgh, PA, Morgantown, WV, and Albany, OR (United States).
- Skone, T. J., Schivley G., Jamieson M., Marriott J., Cooney G., Littlefield J., Mutchek M., Krynock M., Shih C.Y. (2018a) Life Cycle Analysis: Sub-Critical Pulverized Coal (SubPC) Power Plants. (No. DOE/NETL-2018/1888). National Energy Technology Laboratory. Pittsburgh, PA, Morgantown, WV, and Albany, OR (United States), 2018.
- Skone, T. J., Schivley, Greg, J., Matthew, M., Cooney, G., Littlefield, J., Mutchek, M., Krynock, M., and Shih, C. Y. (2018b) Life Cycle Analysis: Supercritical Pulverized Coal (SCPC) Power Plants. (DOE/NETL-2018/1887). National Energy Technology Laboratory. Pittsburgh, PA, Morgantown, WV, and Albany, OR (United States).
- Song, Y., Cervarich, M., Jain, A. K., Kheshgi, H. S., Landuyt, W., and Cai, X. (2016) The Interplay between Bioenergy Grass Production and Water Resources in the United States of America. *Environmental Science & Technology*, 50.6 (2016): 3010-3019.
- Stevens, R., Lewis, E., and McNaul, S. (2021). Comparison of Commercial, State-of-the-Art, Fossil-Based Hydrogen Production Technologies (No. DOE/NETL-2021/2743). National Energy Technology Laboratory, Pittsburgh, PA, Morgantown, WV, and Albany, OR (United States).
- Stolaroff, J. K., Pang, S. H., Li, W., Kirkendall, W. G., Goldstein, H. M., Aines, R. D., and Baker, S. E. (2021). Transport Cost for Carbon Removal Projects with Biomass and CO_2 Storage. *Frontiers in Energy Research*, 9, 639943.
- Tigercat (2024a) 1165 Harvester. Available at https://www.tigercat.com/product/1165-harvester/
- Tigercat (2024b) LH845E Harvester. Available at https://www.tigercat.com/product/lh845e-harvester/
- U.S. Department of Agriculture (USDA). (2022) Agricultural Chemical Use Survey.
- U.S. Department of Agriculture (USDA). (2024). Economic Research Service, National Agricultural Statistics Service, Quickstats. Available at

https://www.ers.usda.gov/topics/crops/wheat/wheat-sector-at-a-glance/#:~:text=Wheat%20ranks%20third%20among%20U.S.,million%20acres%2C%20a%20record%20low
- U.S. Department of Energy (DOE). (2011). U.S. Billion-Ton Update: Biomass Supply for a Bioenergy and Bioproducts Industry. R.D. Perlack and B.J. Stokes (Leads), (No. ORNL/TM-2011/224). Oak Ridge National Laboratory, Oak Ridge, TN. 227p
- U.S. Environmental Protection Agency (EPA). (2007). Methodology for Thermal Efficiency and Energy Input Calculations and Analysis of Biomass Cogeneration Unit Characteristics (No. EPA-HQ-OAR-2007-0012).
- U.S. Environmental Protection Agency (EPA). (2010) Renewable Fuel Standard Program (RFS2) Regulatory Impact Analysis. No. EPA-420-R-10-006.
- Waratch (2024) Harvester Head: H212. Available at https://www.waratah.com/product/h212/
- Winkler, B., Mangold, A., von Cossel, M., Clifton-Brown, J., Pogrzeba, M., Lewandowski, I., Iqbal, Y. & Kiesel, A. (2020). Implementing Miscanthus into Farming Aystems A Review of Agronomic Practices, Capital and Labor Demand. *Renewable and Sustainable Energy Reviews*, 132, 110053.
- WoodsmanPro (2024). Continuous Rotation Tree Harvester 850. Available at https://woodsmanpro.co.nz/woodsman_product/woodsman-pro-850/
- Xuvol (2024). Forestry Tree Harvester. Available at https://xuvol.net/products_html/excavator.html
- Yilmaz, S. (2021). The Relationship between Unburned Carbon Levels in Coal Combustion Ash and Volatile Matter Content in Coal. *Combustion Science and Technology*, 193(4), 716-725
- Zomer, R. J., Bossio, D. A., Sommer, R., and Verchot, L. V. (2017). Global Sequestration Potential of Increased Organic Carbon in Cropland Soils. *Scientific Reports*, 7(1), 15554.
- Zygarlicke, C.J., McCollor, D.P., Eylands, K.E., Hetland, M.D., Musich, M.A., Crocker, C.R., Dahl, J. and Laducer, S. (2001). TASK 3.4 Impacts of Cofiring Biomass with Fossil Fuels. University of North Dakota. Cooperative Agreement No. DE-FC26-98FT4032.

Appendix

Appendix 1 Fuel Property of Coal, Waste Coal, and Biomass.

Table S1.1. Coal Properties.

Coal Rank			**Bituminous**			**Subbituminous**	**Lignite**
Feedstock Name			**Pittsburgh #8 (Appalachian Medium Sulfur)[1]**	**Illinois No.6[2]**	**Upper Freeport (NETL)[3]**	**Wyoming Powder River Basin[4]**	**North Dakota Lignite[5]**
Basis			Dry	As-Received	As-Received	As-Received	As-Received
Fuel Property	Higher Heating Value	kJ/kg	308423	27135	30980	19399	14003
	Carbon	wt.%	73.81	63.75	73.39	48.18	35.04
	Hydrogen	wt.%	4.88	4.5	4.03	3.31	2.68
	Oxygen	wt.%	5.41	6.88	4.79	11.87	11.31
	Chlorine	wt.%	0.06	0.29	0.00	0.01	0.09
	Sulfur	wt.%	2.13	2.51	2.29	0.37	1.16
	Nitrogen	wt.%	1.42	1.25	1.33	0.7	0.77
	Ash	wt.%	7.24	9.7	13.03	5.32	15.92
	Moisture	wt.%	5.05	11.12	1.13	30.24	33.03
Proximate Analysis	Moisture	wt.%	0.00	11.12	1.13	30.24	33.03
	Ash	wt.%	7.63	9.7	13.03	5.32	15.92
	Volatile Matter	wt.%	42.52	34.99	29.43	31.39	27.17
	Fixed Carbon	wt.%	49.86	44.19	56.41	33.05	23.89
Ash Properties	SiO_2	wt.%	54.50	46.80	44.80	63.19	45.16
	Al_2O_3	wt.%	17.30	18.00	24.10	30.00	21.91

	Fe_2O_3	wt.%	4.50	20.00	17.30	2.90	6.97
	CaO	wt.%	10.70	7.00	4.20	0.91	16.42
	MgO	wt.%	2.40	1.00	1.60	0.76	3.26
	Na_2O	wt.%	1.48	0.60	0.00	0.38	0.78
	K_2O	wt.%	1.11	1.90	2.70	1.49	0.80
	TiO_2	wt.%	0.70	1.00	1.30	0.09	1.63
	MnO_2	wt.%	0.00	0.00	0.00	0.00	0.00
	P_2O_5	wt.%	0.27	0.20	0.10	0.08	0.81
	SO_3	wt.%	7.04	3.50	3.90	0.20	1.26
	Other	wt.%	0.00	0.00	0.00	0.00	1.00

Footnotes:
1. Source of Data: IECM (2019a, 2021);
2. Source of Data: NETL (2007);
3. Source of Data: NETL (2019);
4. Source of Data: EPRI (2008);
5. Source of Data: EPRI (2018).

Table S1.2. Waste Coal Properties.

Mining Approach			**Underground**		**Surface**
Feedstock Name[1]			**Herrin Refuse Coal Mach #1**	**Herrin Refuse Coal Lively Grove Coal**	**Dekoven Refuse Coal Eagle River #1**
Basis			As-Received		
Fuel Property	Higher Heating Value	Btu/lb	1777	1985	7522
	Carbon	wt.%	10.47	11.09	39.04
	Hydrogen	wt.%	1.92	2.08	3.37
	Oxygen	wt.%	9.78	9.55	6.36
	Chlorine	wt.%	N/A[2]		
	Sulfur	wt.%	3.57	3.23	9.4

	Nitrogen	wt.%	0.42	0.41	0.93
	Ash	wt.%	73.84	73.64	40.9
	Moisture	wt.%	N/A[2]		
Proximate Analysis	Moisture	wt.%	7.64	7.90	4.67
	Ash	wt.%	73.84	73.64	40.9
	Volatile Matter	wt.%	10.42	9.73	25.05
	Fixed Carbon	wt.%	8.10	8.73	29.38
Ash Properties	SiO_2	wt.%	56.51	61.04	44.51
	Al_2O_3	wt.%	16.07	17.46	14.17
	Fe_2O_3	wt.%	8.70	7.79	30.52
	CaO	wt.%	4.25	0.95	1.62
	MgO	wt.%	1.53	1.64	0.91
	Na_2O	wt.%	0.87	1.16	0.42
	K_2O	wt.%	3.20	2.68	2.10
	TiO_2	wt.%	0.80	0.81	0.77
	MnO_2	wt.%	0.00	0.00	0.00
	P_2O_5	wt.%	0.50	0.37	0.26
	SO_3	wt.%	0.00	0.00	0.00
	Other	wt.%	5.71	5.63	4.17

Footnotes:
1. Source of Data: Kolker et al. (2021);
2. N/A stands for Not-Available.

Table S1.3. Biomass Properties.

Category			Energy Crop					Agricultural Residue				Forestry Residue	
Feedstock Name			**Mechanically Harvested Switchgrass[1]**	**Manually Harvested Switchgrass[1]**	**Miscanthus[2]**	**Hybrid Poplar[3]**	**Torrefied Willow[4]**	**Corn Stover (704)[5]**	**Corn Stover (889)[5]**	**Corn Stover (890)[5]**	**Wheat Straw[6,7]**	**Pine Spruce (3155)[5]**	**Pine Spruce (3156)[5]**
Basis			As-Received				Dry and Ash Free	As-Received			Dry	As-Received	
Fuel Property	Higher Heating Value	Btu/lb	7333	7421	6879	7641	N/A[8]		16230	N/A[8]			
		J/g	N/A[8]				23398[9]	N/A[8]					
		MJ/kg	N/A[8]					17	18.05	13.64	17.9	19.37	19.24
	Carbon	wt.%	40.54	43.55	40.41	45.04	60.30	43.98	44.18	35.57	46.2	48.07	47.78
	Hydrogen	wt.%	5.28	5.13	4.92	6.13	5.80	5.39	5.52	4.55	6.52	5.72	5.43
	Oxygen	wt.%	37.57	37.61	37.19	46.63	33.40	38.85	37.69	32.98	41.43	38.28	35.8
	Chlorine	wt.%	N/A[8]	N/A[8]	0.05	0.01	0.00	0.25	0.00	0.01	0.25	0.01	0.00
	Sulfur	wt.%	0.20	0.10	0.05	0.25	0.00	0.10	0.10	0.08	0.084	0.02	0.04
	Nitrogen	wt.%	0.92	0.79	0.28	0.82	0.52	0.62	0.53	0.61	0.38	0.37	0.84
	Ash	wt.%	5.95	3.93	2.61	1.13	0.00	4.75	6.98	20.3	5.21	1.25	3.79
	Moisture	wt.%	9.53	8.89	14.54	N/A[3]	0.00	6.06	5.00	5.90	N/A[8]	6.30	6.32
Proximate Analysis[10]	Moisture	wt.%	9.53	8.89	14.54	5.20	2.10	6.06	5.00	5.90	6.78	6.30	6.32
	Ash	wt.%	5.95	3.93	2.61	1.13	1.80	4.75	6.98	20.3	5.21	1.25	3.79
	Volatile Matter	wt.%	69.03	81.79	72.12	78.85	66.9	75.96	74.2	60.13	81.44	74.3	69.42
	Fixed Carbon	wt.%	15.49	5.39	10.73	14.82	29.2	13.23	13.82	13.67	13.35	18.15	20.47

Ash Property	SiO_2	wt.%	62.71	48.56	61.84	4.60	N/A[3]	54.04	N/A[3]	N/A[3]	23.35	38.51	27.81
	Al_2O_3	wt.%	8.39	1.08	0.98	1.50		1.99			0.02	4.72	5.67
	Fe_2O_3	wt.%	5.82	0.34	1.35	2.00		N/A[3]			0.55	3.72	2
	CaO	wt.%	4.62	12.77	9.61	49.00		8.66			5.66	15.39	11.89
	MgO	wt.%	3.65	20.41	2.46	8.50		6.11			0.36	3.98	1.82
	Na_2O	wt.%	0.59	2.38	0.33	0.40		0.15			0.91	0.31	1.44
	K_2O	wt.%	1.95	2.92	11.60	24.90		20.67			40.32	8.31	4.1
	TiO_2	wt.%	0.53	0.07	0.05	0.10		N/A[8]			0.18	0.5	0.35
	MnO_2	wt.%	N/A[8]	N/A[8]	0.00	0.00					0.00	N/A[8]	N/A[8]
	P_2O_5	wt.%	2.73	5.89	4.20	7.80		8.68			4.01	3.21	1.76
	SO_3	wt.%	2.28	3.83	2.63	1.20		N/A[8]			3.83	1.62	1.35
	Other	wt.%	N/A[8]	N/A[8]	4.95	0.00					20.80	N/A[8]	N/A[8]

Footnotes:
1. Source of Data: Bush et al. (2001);
2. Source of Data: EPRI (2010);
3. Source of Data: Zygarlicke et al. (2001);
4. Source of Data: Bridgeman et al. (2010);
5. Source of Data: ECN (2022);
6. Source of Data: EPRI (2012);
7.The ash property is calculated based on the ICP-OES ssh elemental analysis result;
8. N/A stands for Not-Available;
9. The heating value is dry basis;
10. The proximate analysis data is on an as-received basis.

Table S1.4. Willow Ash Properties.

Category			**Energy Crop**										
Sample Number (No.)[1]			**719**	**1305**	**1306**	**1307**	**851**	**852**	**867**	**868**	**869**	**870**	**720**
Ash Property	SiO_2	wt.%	8.08	2.30	27.40	2.00	16.76	2.83	1.11	1.89	2.35	1.82	2.05
	Al_2O_3	wt.%	1.39	0.35	2.60	0.30	3.01	0.12	0.09	0.16	1.41	1.48	1.97
	Fe_2O_3	wt.%	0.84	0.33	1.40	0.20	0.85	0.42	0.21	0.30	0.73	0.49	0.35

	CaO	wt.%	45.62	37.2	25.1	37.5	34.86	36.51	40.48	32.00	41.2	44.68	34.18
	MgO	wt.%	1.16	4.80	4.10	5.10	2.46	1.54	3.04	7.67	2.47	2.16	2.98
	Na_2O	wt.%	2.47	2.80	2.50	2.90	3.05	1.97	0.77	0.65	0.94	0.86	2.67
	K_2O	wt.%	13.20	12.10	10.10	12.80	12.20	19.90	13.90	22.10	15.00	15.30	18.40
	TiO_2	wt.%	0.06	0.03	0.15	0.02	0.07	0.06	0.00	0.04	0.05	0.05	0.03
	MnO_2	wt.%	N/A[2]										
	P_2O_5	wt.%	10.04	10.2	7.30	10.8	10.36	12.9	8.16	11.68	7.40	7.18	7.10
	SO_3	wt.%	1.15	3.20	2.60	3.60	1.70	1.94	1.70	3.09	1.83	2.33	2.92
	Other	wt.%	13.67	2.95	1.30	2.50	17.58	19.85	27.10	17.65	18.24	18.34	22.64

Footnotes:
1. Source of Data: ECN (2022);
2. N/A stands for Not-Available.

Table S1.5. Energy-Based Biomass Feedstock Cost.

Biomass Type	**Energy Crop**						**Agricultural Residue**	**Forest Residue**		**Wood Waste**
	Poplar	**Switchgrass and other**	**Miscanthus**	**Bagasse**	**Sorghum**	**Willow**		**Pine Residues**	**Hardwood Residues**	
Cost[1] (2014$/MMBtu)	1.5–3.6	2.4–3.4	2.8–8.2	2.2	2.3–2.9	3.1–3.4	1.4–3.5	1.2–1.5	0.9–1.4	1.1–3.2

Footnote:
1. Source of Data: IRENA (2015).

Table S1.6. Transport Cost.

Transport Method	**Truck**	**Train**
Cost (2017$/tonne/km)[1]	0.10	0.04

Footnote:
1. Source of Data: Stolaroff et al. (2021).

Appendix 2 Global Warming Potential Value and Emission Intensity Associated with Consumption of Electricity, Diesel, and Steel.

Table S2.1. 100-Year Global Warming Potential (GWP).

Greenhouse Gas	GWP Value[1]	Unit
CO_2	1	kg CO_2eq
CH_4	36	kg CO_2eq
N_2O	298	kg CO_2eq

Footnote:
1. Source of Data: IPCC (2014).

Table S2.2. Emission Intensity Associated with Electricity Consumption (E_e).

Greenhouse Gas	Emission Intensity[1]	Unit
CO_2	5.47E+02	kg CO_2/MWh
CH_4	1.04E+00	kg CH_4/MWh
N_2O	6.92E-03	kg N_2O/MWh

Footnote:
1. Source of Data: NETL (2023).

Table S2.3. Emission Intensities of Diesel Production and Combustion (E_{diesel}).

Greenhouse Gas	Diesel Production[1]	Diesel Combustion[2]	Unit
CO_2	6.26E-01	3.08E+00	kg CO_2/kg_{diesel}
CH_4	4.19E-03	1.05E-04	kg CH_4/kg_{diesel}
N_2O	1.21E-05	1.21E-05	kg N_2O/kg_{diesel}

Footnotes:
1. Source of Data: NETL (2011a);
2. Source of Data: NETL (2014).

Table S2.4. Emission Intensity Associated with Steel Consumption (E_{steel}).

Greenhouse Gas	Emission Intensity[1]	Unit
CO_2	2.2E+00	kg CO_2/kg_{steel}
CH_4	5.1E-03	kg CH_4/kg_{steel}
N_2O	2.7E-06	kg N_2O/kg_{steel}

Footnote:
1. Source of Data: NETL (2016).